Hippocampus

WILEY

RESEARCH ARTICLE

Ketamine Sustains and Enhances the Protective Effects of a Ketogenic Diet Against Relapses in an Anorexia Mouse Model

Yiru Dong[1] | Jundi Wang[1] | Olivia Ge[1] | Yuki Lin[1] | Chiye Aoki[1,2]

[1]Center for Neural Science, New York University, New York, USA | [2]NYU Langone School of Medicine, The Neuroscience Institute, New York, USA

Correspondence: Chiye Aoki (ca3@nyu.edu)

Received: 28 May 2025 | **Revised:** 14 September 2025 | **Accepted:** 22 September 2025

Funding: This work was supported by the Vulnerable Brain Project; Baszucki Group; New York University.

Keywords: activity-based anorexia | anorexia nervosa | exercise | food restriction | food-anticipatory activity | ketamine | ketogenic diet | ketone bodies | wheel running

ABSTRACT

Anorexia nervosa (AN) has high mortality and relapse rates, yet no accepted pharmacotherapies. Reports based on six individuals suggest that ketogenic diet (KGD) combined with sub-anesthetic ketamine (KET) is an effective treatment. The animal model, Activity-Based Anorexia (ABA), captures AN's maladaptive behaviors of voluntary food restriction, excessive exercise, severe weight loss, heightened anxiety and relapse vulnerability. Using ABA, we tested whether (1) KGD, alone, can protect against relapses after a severe anorexia-like experience; (2) KGD must be maintained to prevent relapses; (3) sub-anesthetic KET combined with KGD is more ameliorative than KGD alone. We also (4) explored KGD's mechanism for protecting against relapses by electron microscopic (EM) analysis of synapses in the hippocampus. To simulate AN relapses, we imposed ABA induction twice (ABA1, ABA2), with 10 recovery days in between. Animals were fed a standard diet (SD, pellet plus wet food) during ABA1 and KGD during ABA2 (SD➔KGD). ABA vulnerability, measured by food restriction-evoked hyperactivity and weight loss, was severe during ABA1 but significantly less during ABA2, compared to those fed SD throughout ABA1 and ABA2 (SD➔SD). KGD withdrawal after ABA1 (KGD➔SD) caused vulnerability during ABA2 to become as severe as for the SD➔SD, indicating that KGD must be maintained to be protective. We tested whether KET plus KGD during ABA1 can protect against ABA2 relapse in the absence of KGD or KET (KGD + KET➔SD). During ABA2, KGD + KET➔SD exhibited low maladaptive behaviors, similarly to those maintained on KGD throughout ABA1 and ABA2 (KGD➔KGD), with greater weight during recovery. Thus, KET sustains and boosts KGD's benefits for > 10 days, supporting clinical findings that short-term KGD + KET may be an effective treatment for preventing AN relapses. EM revealed that KGD increases GABAergic synapse lengths and may reduce ABA vulnerability by increasing excitatory synaptic drive of GABAergic interneurons and increasing E-to-E synapses' role in body weight regulation.

1 | Introduction

Anorexia nervosa (AN) is a mental disorder characterized by compulsive self-imposed food restriction, severe weight loss, body dysmorphia (APA 2013), and excessive exercise (Beadle et al. 2015; Beumont et al. 1994; Carrera et al. 2012; Davis et al. 1997; Hebebrand et al. 2003; Kron et al. 1978). AN has one of the highest mortality rates among mental disorders

Yiru Dong and Jundi Wang share first-authorship.

(Arcelus et al. 2011; Birmingham et al. 2005), due to severe medical complications affecting multiple organ systems (Mehler and Brown 2015) and high suicide rates (Smith et al. 2018). Unlike other mental disorders, no established pharmacotherapy exists for the initial onset of AN or relapses (Crow 2019). AN is frequently associated with pre-existing anxiety (Dellava et al. 2010; Kaye et al. 2009); yet, unlike obsessive-compulsive disorders and major anxiety disorders, anxiolytic medications have limited efficacy (Steinglass et al. 2014). While atypical antipsychotics have continued to be developed for schizophrenia and bipolar disorder, their benefits in treating AN are modest (Fornaro et al. 2023; Hillebrand et al. 2005). Cognitive behavioral therapies have shown the greatest efficacy (Dalle Grave et al. 2014; Galsworthy-Francis and Allan 2014; Mulkens and Waller 2021), but individuals who continue to experience AN into adulthood face unacceptably higher risks of relapses compared to those who recover during adolescence (> 30%) (Berends et al. 2018; McFarlane et al. 2008; Walsh 2013).

Our long-term goal has been to explore the etiology of AN and its relapses, especially in adulthood, through the activity-based anorexia (ABA) animal model (Routtenberg and Kuznesof 1967). Although ABA does not capture a core feature of AN—body dysmorphia—ABA replicates five key remaining symptoms of AN: excessive exercise, severe weight loss, voluntary food restriction, relapses, and heightened anxiety, each of which can be quantified to assess individual differences in ABA vulnerability during the first onset and during relapses (Aoki 2020; Aoki and Santiago 2022; Chowdhury et al. 2013; Wable, Min, et al. 2015). ABA is readily induced by combining wheel acclimation with restricted food access (Aoki 2020). This combination evokes heightened exercise on a wheel, likely mimicking innate foraging-like behavior that is triggered by hunger in animals and humans (Gutierrez 2013). While foraging is adaptive in the wild, continuous wheel running in captivity is maladaptive. When re-exposed to restricted food access (ABA2), following the first induction of anorexia-like behavior during ABA1, some mice again exhibit rapid weight loss due to wheel running and voluntary food restriction (FR), demonstrating relapse vulnerability, while others exhibit gain of resilience by suppressing food restriction-evoked hyperactivity. This reduction of food restriction-evoked hyperactivity contributes to relatively better weight retention (Chowdhury et al. 2013).

A series of studies leading up to this report pointed to the central role of GABA in the hippocampus as being associated with the gain of resilience: those individuals that exhibit greater GABAergic inhibition of pyramidal cells in the hippocampus, measured as augmented GABAergic innervation (Chowdhury et al. 2019, 2013), larger inhibitory synaptic currents (Chowdhury et al. 2019), and heightened $GABA_A$ receptor expression (Aoki et al. 2018; Chen et al. 2018; Wable et al. 2014; Wable, Chen, et al. 2015) were the same animals that gained ABA resilience. Those animals that gained ABA resilience modestly following ketamine treatment in adulthood also showed a trend towards increased GABAergic innervation in the hippocampus (Dong and Aoki 2025; Goodwin-Groen et al. 2023). The tight correlation between ABA resilience and GABAergic synapse strengths in the hippocampus may be due to this brain region's central role in anxiety regulation and cognition (Aoki and Santiago 2022; Shen et al. 2007, 2005, 2010).

Genome-wide association studies suggest that AN has metabopsychiatric origins, linking it to BMI-lowering alleles and genetic traits associated with obsessive-compulsive disorder, anxiety, and schizophrenia, among others (Duncan et al. 2017; Watson et al. 2019). The high-fat/low-carbohydrate ketogenic diet (KGD) shows potential as a treatment for AN by addressing both its metabolic and neurological components—normalizing metabolic pathways, as observed in diabetic patients (Paoli et al. 2023), and stabilizing neuronal excitability, as seen in epilepsy treatments (D'Andrea Meira et al. 2019; Vining et al. 1998; Wilder 1921). Case reports totaling nine adults diagnosed with AN indicate that KGD leads to remission lasting multi-months (Calabrese et al. 2022) to multi-years (Norwitz et al. 2023; Scolnick et al. 2020). However, six of the nine AN cases in these reports combined KGD with sub-anesthetic ketamine, leaving unanswered whether KGD alone can ameliorate AN. Using the ABA animal model, KGD alone was shown to decrease weight loss of 26 adult female mice during the first onset and relapses of anorexia-like behavior, so long as animals were maintained on KGD (Dong et al. 2024). The current study used the ABA model to address four lingering questions: (1) Can KGD ameliorate *relapses*, if introduced during ABA2, rather than prior to ABA1? (2) Does the sustained benefit of KGD require sustained adherence to KGD? (3) Does ketamine aid in sustaining KGD's ameliorative effects? and (4) Does enhanced GABAergic inhibition and/or changes in glutamatergic synapses in the hippocampus contribute to KGD's ameliorative properties?

2 | Method

2.1 | Animals

All procedures were ethically reviewed and approved and in accordance with the NIH Guide for the Care and Use of Laboratory Animals and approved by the IACUC of New York University (A3317-01). All procedures are compliant with the US National Research Council's Guide for the Care and Use of Laboratory Animals, the US Public Health Service's Policy on Humane Care and Use of Laboratory Animals, and the Guide for the Care and Use of Laboratory Animals.

All animals were born at the animal facility of New York University. All were of C57BL6 background, with some from non-phenotypic Cre-only or loxp-only knock-in stocks of Jackson Laboratory. We verified no difference in FR-evoked hyperactivity, weight, or food consumption across these stocks (Dong and Aoki 2025; Dong et al. 2024; Goodwin-Groen et al. 2023). Cohort effects were minimal, and no data were excluded. Both males and females were included in the study, based on recent evidence that eating disorder is on the rise among males (Gorrell and Murray 2019).

2.2 | The ABA Procedure

Figure 1a shows the timeline of 2 cycles of ABA. In brief, all animals were housed in a room with lights on from 7 am to 7 pm, with controlled ambient temperature and humidity (Figure 1b). Each ABA cycle began with wheel acclimation for 5 days. This

was followed by three to 4 days of food restriction (FR), during which wheel access was ad libitum and food access became limited to 2 h per day, from 7 to 9 pm (Figure 1b) but unlimited in amount. This was followed by 4 to 5 days of recovery, during which food access returned to be ad libitum and the wheel was removed. For animals undergoing relapses, the last day of recovery was followed immediately by the wheel acclimation phase of the next ABA cycle, that is, ABA2 or ABA3. Further details are available in the Figure 1 legend and a previous publication (Aoki 2020).

2.3 | Diet

Animals allocated to the KGD were fed commercially prepared ketogenic paste (Bio-Serve Cat #F3666, 7.24 kcal/g, with 93.4% of the total kcal from fat, 1.8% from carbohydrate, 4.7% from protein), provided in a cup on the floor for no less than 10 days before FR started. This was to ensure that animals had reached ketosis by the time FR began (Dong et al. 2024). Animals fed a standard diet (SD) received rat chow pellets (3.02 kcal/g, 13.12% kcal from fat, 24.5% from protein, 62.4% from carbohydrates) plus balanced wet food in a cup (Clear H_2O DietGel 76A, 1 kcal/g, 18% of the calories from fat, 17% of the calories from protein, 65% of the calories from carbohydrates). The reason for adding wet food in cups was to provide choices for animals to eat and hydrate readily during the shortened period of food availability of subsequent FR days. For animals transitioning from SD to KGD, such as on the first day of recovery from ABA1 under SD, all three types of food—rat chow pellets, wet food, and KGD paste—were given to ensure that the transition did not cause animals to experience another day of food deprivation due to food neophobia (Modlinska et al. 2015). All animals were given a wooden block to mitigate teeth overgrowth that can accompany the KGD paste-only environment.

2.4 | The Schedule of Weight and Food Measurements During ABA

On non-FR days, when food was available ad libitum, body weight and food weights were measured once per day at around 1 pm.

On FR days, food was only available from 7 pm to 9 pm. To animals fed SD, a cup containing wet food was placed on the floor and a hopper filled with pellets was placed within the cage at 7 pm. At 9 pm, both pellets and wet food were removed and replaced by an empty hopper and a Hydrogel water cup (Clear H2O Hydrogel #70-01-5022, 0 Kcal/g). To animals fed KGD, a cup containing KGD paste was placed on the floor together with an empty food hopper. At 9 pm, the cup containing KGD was replaced with a Hydrogel water cup and the hopper remained empty. Body weights and food weights were measured at 7 pm and 9 pm. Additionally, on the first day of FR (FR1), body weights and food weights were measured additionally at 1 pm, just prior to the removal of food. To ensure complete food restriction from 9 pm until 7 pm of the next day, soiled bedding material and food crumbs were removed at 1 pm on FR1 and nightly at 9 pm on FR days, without removing the nesting material.

Food consumption on FR days was measured based on decreased weight of food at 9 pm, compared to the food weight at 7 pm. On non-FR days, food consumption was measured based

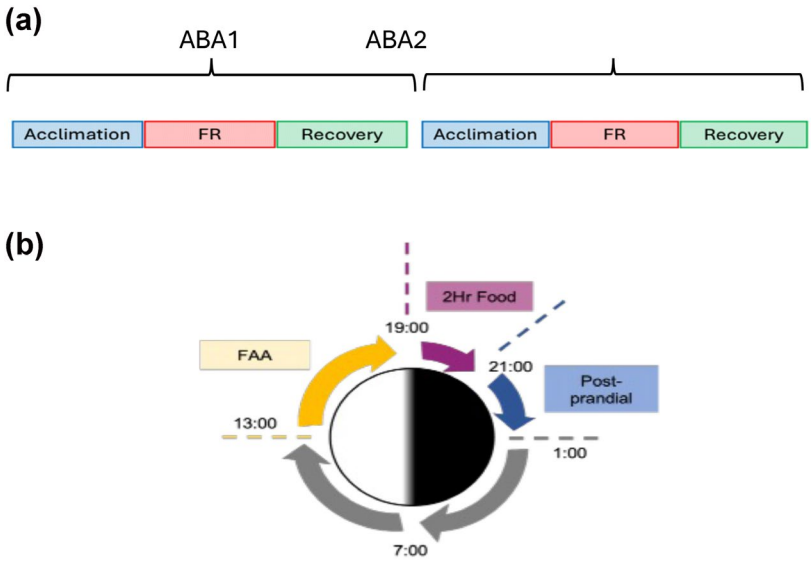

FIGURE 1 | (a) Schema of ABA cycles. Acclimation lasts for 4–5 days, during which period animals acclimate to a running wheel placed in its cage. FR are the food-restricted days, beginning at 1 pm and lasting 3 to 4 days. During FR, wheel access is ad libitum, while food access is restricted to 2 h per day. Recovery lasts for 4–5 days, during which period animals eat ad libitum in the absence of a wheel. This ABA cycle was repeated 2 to 3 times. (b) Names of time zones on FR days. "FAA" is food-anticipatory activity hours, 13–19 (1 pm-7 pm), spanning the 6 h leading up to the feeding hours. "2 Hr Food" indicates hours of food access, limited to 19–21 (7 pm—9 pm). Post-prandial dark hours are 21–1 (9 pm-1 am). The remaining hours are divided into two: Dark 1–7 (1 am-7 am) and Light 7–13 (7 am-1 pm). (c) Dietary schedules spanning multiple cycles of ABA. Pink lines depict days when the standard diet of rat chow pellet plus wet food is fed. Blue lines depict days when KGD is fed. Purple depicts days when animals are fed a combination of SD and KGD, when the diet schedule transitions from KGD to SD or from SD to KGD. Syringes indicate days when ketamine was injected.

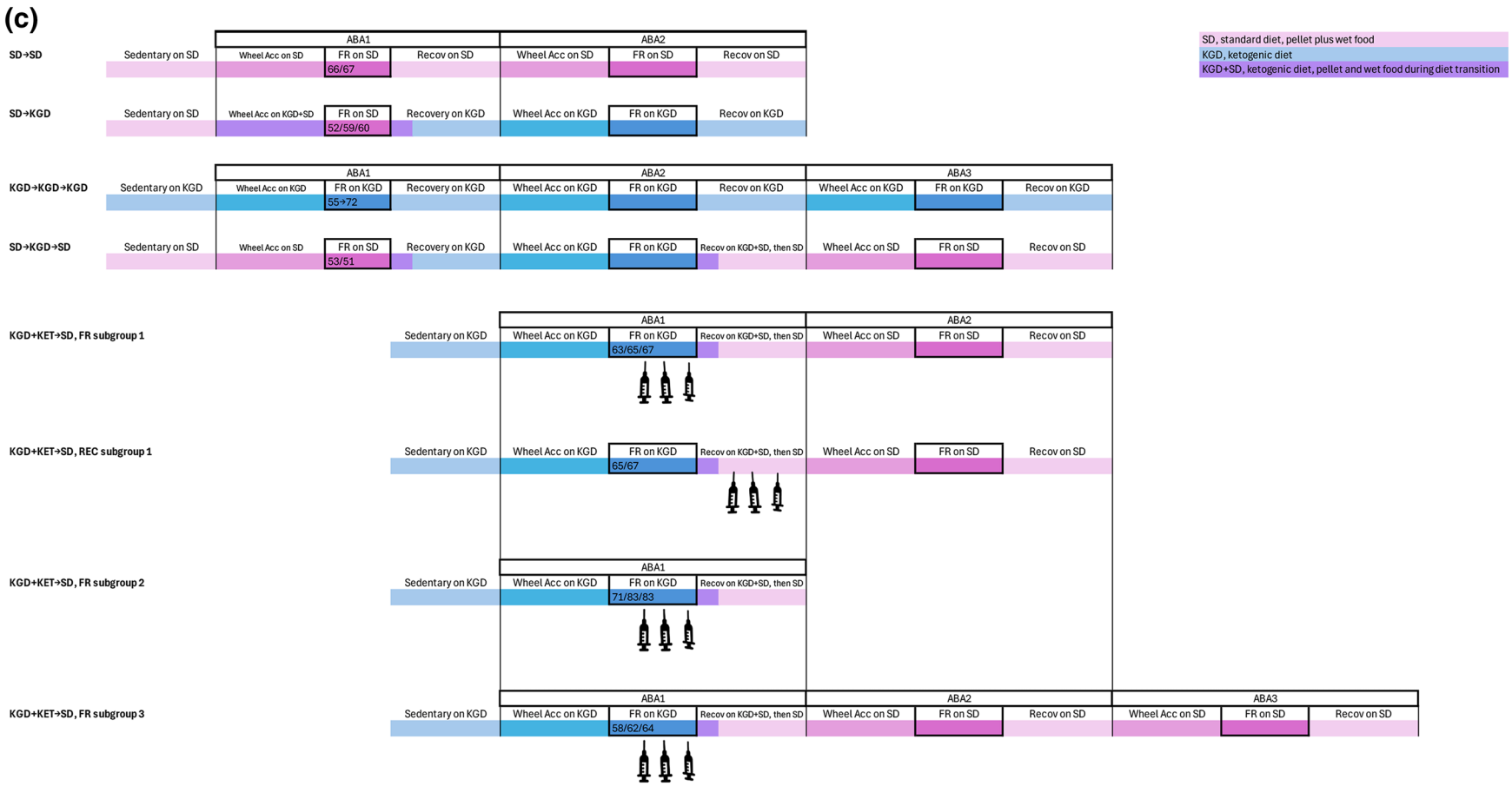

FIGURE 1 | (Continued)

on food weights at 1 pm, relative to food weight the day before. Food weights were then converted to Kcal.

2.5 | Normalization of Food Consumption and Body Weights

Since food consumption is dependent on body weight, which varied greatly across individuals within and across the sex subgroups and increased from ABA1 to ABA2, food consumption of each animal was normalized to its own baseline intake, averaged over the 2 days leading up to 1 pm of FR1 of ABA1 and ABA2. Body weights were normalized to the average of body weights on the 2 days that preceded FR, namely the values at 1 pm on FR1 and 1 pm of the day before FR1 (= Acc1).

2.6 | Schedules of ABA1, ABA2, and ABA3 Under Varying Diet Conditions

Figure 1c shows the timeline of various ABA cycle schedules that animals underwent. The color scheme highlights the differences in diet. The number of days of acclimation, FR, and recovery of ABA cycles was kept constant across cohorts with varying diet conditions.

The SD➔SD group ($N = 17$, 10 females) was fed a standard diet comprised of pellets and wet food (pink) across ABA1 and ABA2.

The SD➔KGD group ($N = 16$, 7 females) was fed a combination of SD and KGD (purple) during the 5 days preciding ABA1 (Acc) to avoid food neophobia, then fed just the SD (pink) during FR1, FR2, and FR3 of ABA1, followed by the combination of SD and KGD for one reovery day, then only KGD during the remaining 4 days of recovery from ABA1 and during all of the wheel re-acclimation days. They were fed KGD (blue) during FR1 through FR4 of ABA2 and recovery days following ABA2.

The KGD➔KGD group ($N = 19$, 17 females) was fed KGD (blue) across ABA1, ABA2, and ABA3.

The KGD➔SD group ($N = 17$, 9 females) was fed SD (pink) during ABA1, ABA3, and KGD (blue) during ABA2.

The KGD + KET➔SD group ($N = 26$, 10 females) was fed KGD (blue) during ABA1, while receiving ketamine treatment, but SD (pink) and no ketamine treatment during ABA2. The KGD + KET➔SD➔SD group ($N = 9$, 9 females) was fed KGD (blue) during ABA1, while receiving ketamine treatment, and SD (pink) without ketamine treatment during ABA2 and ABA3.

2.7 | Ketamine Treatment of the KGD + KET➔SD Group

Thirty-five animals of the KGD + KET group, distributed across three cohorts, received intraperitoneal (IP) injections of ketamine during FR days 2, 3, 4 (FR2, FR3, FR4) of ABA1 (KGD + KET-FR subgroup, $N = 27$) or during Recovery days 2, 3, 4 (Recov2, Recov3, Recov4) that followed ABA1 (KGD + KET REC-subgroup, $N = 8$, 5 females) (see Figure 1c). To acclimate animals to IP injections, all animals were mock-injected once per day at 4:30 pm for 3 days prior to the first FR day of ABA1 (ABA1FR1). Mock injection involved picking up the animal and gently touching the abdomen with a syringe lacking a needle. At exactly 4:30 pm on FR1 of ABA1, all animals received an IP injection of vehicle (1% mL/kg of sterile saline). On FR2 of ABA1, 27 animals assigned to the KGD + KET FR-subgroup received a 30 mg/kg IP ketamine injection in a volume of 1% mL/kg at 4:30 pm. This procedure was repeated for FR3 and FR4 of ABA1 for all animals of the KGD + KET FR-subgroup. Eight animals that were assigned to the KGD + KET REC-subgroup received 30 mg/kg ketamine IP in a volume of 1% mL/kg at 4:30 pm on Rec2, Rec3, and Rec4 following the FR days of ABA1.

In a pilot study, a one-way ANOVA was conducted to assess whether ketamine injection during FR days (KGD + KET➔SD, FR-subgroup $N = 10$) versus recovery days (KGD + FR➔SD, Recov-subgroup, $N = 8$) yielded different behavioral effects. This analysis yielded no group difference for the total wheel activity averaged across FR days 2, 3, and 4 ($p = 0.998$ for ABA1, $p = 0.993$ for ABA2), FAA (food anticipatory activity) averaged across FR days 2, 3, and 4 ($p = 0.790$ for ABA1; $p = 0.710$ for ABA2), the normalized food consumption averaged across FR days 2, 3, and 4 ($p = 0.985$ for FR days of ABA1; $p = 0.937$ for Recovery days of ABA1, $p = 0.937$ for FR days of ABA2; $p > 0.999$ for Recovery days of ABA2), or for normalized body weights on FR days, averaged across FR days 2, 3, and 4 ($p > 0.996$ for ABA1 at 7 pm; $p = 0.960$ for ABA1 at 9 pm; $p = 0.801$ for ABA2 at 7 pm; $p = 0.945$ for ABA2 at 9 pm). There was an isolated group difference for the recovery body weight following ABA1 ($p = 0.017$, with 4% greater weight retention for the FR-subgroup) and no group difference for the recovery body weight following ABA2 ($p = 0.823$). Based on these comparisons, behavioral data from the two sub-groups of the KGD + KET➔SD were combined when comparing to the behavior of the KGD➔KGD and KGD➔SD groups.

Our earlier work had shown that IP injection of saline, administered identically as described for the KET injections during FR days of animals fed only SD, yielded no difference in behavior compared to those without IP injections of saline and also fed SD (Dong and Aoki 2025; Goodwin-Groen et al. 2023). Specifically, two-way ANOVA with Tukey's multiple comparisons test revealed no significant difference for wheel activity ($p = 0.795$ during ABA1 with or without IP saline injection; $p = 0.485$ for the subsequent ABA2 with no injection for either group), food consumption ($p = 0.321$ for ABA1, $p = 0.437$ for ABA2), or lowest weight during the FR period ($p = 0.694$ during ABA1; $p = 0.105$ for ABA2, with 2% greater weight for the non-injected SD group). This indicated that the SD➔SD group with and without vehicle injections could be combined for behavioral analyses and that the KGD + KET➔SD group's behavior could be compared to those of KGD➔KGD and KGD➔SD that did not experience IP injections.

2.8 | Elevated Plus Maze Test (EPM)

EPM was conducted upon all animals to quantify anxiety- and exploration-like behaviors after recovery from the last ABA cycle,

TABLE 1 | Summary of the SLM parameters quantified.

IDs of KGD group	Area of synaptic neuropil surveyed (μm^2)	Number of GABAergic dendrites analyzed	Number of axo-spinous profiles encountered	Number of GABAergic axons analyzed
W1 28,826	873	50	441	107
W2 28,808	1014	35	498	97
W4 28,811	1319	43	786	100
W7 28,813	594	34	315	116
W8 28,825	688	56	263	114
IDs of SD group	**Area of synaptic neuropil surveyed (μm^2)**	**Number of GABAergic dendrites analyzed**	**Number of Axo-spinous profiles encountered**	**Number of GABAergic axons analyzed**
W8 29,733	1033	32	338	95
W10 29,732	1565	71	895	104
W11 28,806	656	26	261	103
W12 29,731	856	63	470	100
W14 29,729	823	44	430	100

1–2 days before euthanasia and after their weights were fully restored. EPM duration was 10 min. The time spent in the open arms and frequency of entering the open arms were recorded and analyzed using the EthoVision XT13's tracking system (Noldus Information Technology, Wageningen, the Netherlands).

2.9 | Euthanasia

Euthanasia at the end of the experiment was performed a few days after EPM tests. Animals were deeply anesthetized using urethane (34%, 0.2–0.3 cc/20 g), during which time animals were transcardially perfused with 20 mL of phosphate-buffered saline, pH 7.4, containing 1 U/mL of heparin, followed immediately by perfusion with 250 mL of 4% paraformaldehyde in 0.1 M phosphate buffer (pH 7.4), all at a rate of 25 mL/min.

2.10 | Tissue Processing for Electron Microscopy

Multiple vibratome sections (50 μm thick) were prepared from the dorsal hippocampus of each animal's brain in the coronal plane. These sections were incubated for 1 h at room temperature under constant agitation in a blocking buffer containing 0.01 M phosphate buffer/0.9% sodium chloride (PBS, pH 7.4), supplemented with 1% bovine serum albumin (BSA, w/v; Sigma Chem., St. Louis, MO), 0.05% sodium azide (w/v; Sigma Chem.). Then, sections were incubated overnight in blocking buffer containing the anti-GAD67 antibody (MAB5406, Millipore, originally Chemicon mouse monoclonal 1G10.2, RRID AB_2278725, 1:800 dilution). Following incubation in anti-GAD, sections were rinsed in PBS for 15 min and then incubated for 1 h at room temperature in PBS/BSA/azide buffer containing biotinylated goat anti-mouse IgG (1:200; Vector Inc., Burlingame, CA). After an additional 30-min PBS rinse, sections were incubated for 30 min in PBS containing the avidin-biotinylated horseradish peroxidase complex (ABC; Vector's ABC Elite Kit) under constant agitation. The sections were then rinsed in PBS and reacted with the peroxidase substrate, 3,3′-diaminobenzidine hydrochloride (DAB; 10 mg per 44 mL PBS) with 4 μL of 30% hydrogen peroxide, terminating the reaction after 13 min with repeated PBS rinses.

Following immunocytochemical processing, sections were post-fixed while free-floating in multi-wells with 1% glutaraldehyde (EMSciences) in PBS, then with 1% osmium tetroxide buffered with 0.1 M phosphate buffer for 1 h, dehydrated in graded ethanol solutions up to 70%, and post-fixed for 1 h with 3% uranyl acetate in 70% ethanol. Dehydration continued to 100% ethanol, followed by acetone rinsing and infiltration with EPON 812. Tissue was embedded between two Aclar plastic sheets with lead weights to ensure flatness and cured at 60°C. The flat-embedded vibratome sections were re-embedded in Beem capsules filled with EPON 812, then ultrathin-sectioned tangentially. Due to the natural curvature of each section, at least 10 ultrathin sections were collected to ensure sampling of the surface-most regions, where immunoreactivity was expected to be maximal, across the anatomical layers of the CA1 hippocampus. These sections were mounted on 400-mesh thin-bar nickel grids, then viewed using JEOL XL1200 without counterstaining with lead citrate, to maximize detection of HRP reaction products. All EM reagents were purchased from EMSciences (Hatfield, PA) unless specified otherwise.

2.11 | Quantitative Electron Microscopic Analyses

Quantitative analysis was conducted to evaluate the extent of inhibitory symmetric synapses formed by GAD-immunopositive (GAD+) axon terminals on the plasma membrane of pyramidal cells in the dorsal hippocampal CA1 field. Due to limitation in human resources, we prioritized our EM study by analyzing only brains of females of the SD➔SD ($N = 10$) and SD➔KGD ($N = 7$). Pyramidal neurons' cell bodies within the pyramidal cell layer (PCL) were identified at a magnification of 12,000×, based on morphological criteria, including a round nuclear membrane, minimal nuclear

membrane indentations, a relative lack of euchromatin, absence of asymmetric (excitatory) synapses on their plasma membrane, and absence of GAD-immunoreactivity. Glial cells in PCL were distinguished by the presence of dense chromatin along the inner rim of the nuclear envelope, while cell bodies of GABAergic interneurons were characterized by a highly indented nuclear membrane, the presence of asymmetric (excitatory) synapses on their plasma membrane, and GAD-immunolabeling throughout the cytoplasm.

We also analyzed GABAergic dendritic shafts and GABAergic axon terminals forming synapses onto dendrites of pyramidal neurons and GABAergic neurons in stratum lacunosum-moleculare (SLM) at a magnification of 25,000×. GABAergic dendrites were characterized by the presence of asymmetric (excitatory) synapses on flat (non-spinous) dendritic shaft plasma membranes, paucity of dendritic spines, paucity of vesicles, presence of microtubules, and GAD-immunolabeling, especially along the inner surface of plasma membranes. We quantified the number and lengths of excitatory (E) and inhibitory (I) synapses formed onto GABAergic (I) and pyramidal cell (E) dendrites (E-to-I, I-to-E, I-to-I). We also quantified the number of E-to-E synapses, that is, axo-spinous synapses formed between immuno-negative axon terminals and immune-negative dendritic spines of pyramidal neurons, with thick postsynaptic densities (PSD) along the inner surface of the plasma membrane of spines at the point of contact. These values were normalized across brain samples in three ways, based on (1) neuropil area surveyed, (2) frequency of encounter with all GAD+ axons (synaptic or not) and all (3) frequency of encounter with GAD+ dendrites (synaptic or not).

For off-line analyses, AMT's XR80 CCD camera system (Boston, MA), attached to a JEOL 1200XL electron microscope with software developed by AMT, was used. To quantify the extent of GAD+ synapses on pyramidal cells and GAD+ dendrites and the extent of glutamatergic synapses onto GAD+ dendrites, the lengths of each GABAergic dendrite's plasma membrane and synapse lengths of GAD+ and GAD- axon terminals were measured using the segmented line tool of ImageJ (FIJI version 2.1.0/1.53c). For measurements involving pyramidal cell bodies, this procedure was followed by measurement of the summed lengths of GAD+ inhibitory synapses along its plasma membrane, to calculate the percentage of plasma membrane contacted by GAD+ axon terminals.

2.12 | Sampling of EM Images

To ensure optimal immunolabeling, only cell bodies, axons, and dendrites located within ultrathin sections at the transition between the vibratome section surface and resin were included in the analysis. Neuronal profiles residing at the tissue-resin interface were examined in the strict order of encounter to minimize sampling bias. The number of analyzed pyramidal cell bodies per animal ranged from 8 to 10, with most animals contributing data from 10 cells.

For five of the KGD and five of the SD-fed animals, we also analyzed the frequency of encounter with inhibitory and excitatory synapses in SLM. For this analysis, a minimum of 10 GABAergic dendritic shafts and approximately 100 GABAergic axon terminals spanning SLM per animal were analyzed (Table 1). The areal density of excitatory synapses surrounding these GABAergic dendrites and axons was also assessed. The area of synaptic neuropil surveyed, the number of GABAergic axons and dendrites analyzed, and the number of axo-spinous profiles encountered appear in Table 1. For the analysis of E-to-I synapses (excitatory inputs to GABAergic dendrites), we assessed the proportion of all GABAergic dendrites encountered that received excitatory inputs. For each animal, this proportion was assessed repeatedly for neuropil area encompassing 5 electron micrographs, equal to 210 μm^2. Investigators responsible for capturing electron microscopic images and performing ImageJ (Fiji) analysis were blind to the animals' wheel-running activity, weight, food intake, and anxiety-like behavior.

2.13 | Statistical Analyses

Data points are missing occasionally due to mechanical problems with wheel activity acquisition, days missed in recording body and food weights, death or removal of animals from the study when they lost > 20% of baseline body weight. We performed two-way ANOVA, with drug/food treatment and time as two factors, allowing for mixed effects analysis for missing data points, followed by Tukey's or Bonferroni correction for multiple comparisons and adjusted p values. For each of the ABA vulnerability measurements, we performed one-way ANOVA across three experimental groups (KGD➔KGD, KGD + KET➔SD, KGD➔SD). For comparing behavior and EM data of SD➔SD versus SD➔KGD groups, we performed unpaired t-tests. Behavioral data of SD➔SD and SD➔KGD groups were correlated with biometric measurements using the Pearson correlation tests. All tests were two-sided, and alpha levels were set at $p < 0.05$. For survival curves, curve comparisons used the Log-rank (Mantel-Cox) test. Statistical tests and graphical representations were prepared using Prism (GraphPad version 10).

2.14 | Preparation of Figures

Graphs were prepared using Prism (GraphPad version 10). Electron micrograph plates were prepared using Adobe Photoshop 2025 version or ImageJ.

3 | Results

3.1 | Testing the Efficacy of Delayed KGD Treatment for ABA Relapses

A previous study showed that KGD ameliorated ABA's maladaptive behaviors, quantified as a reduction of food restriction-evoked hyperactivity, severe weight loss, and grimacing (Dong et al. 2024). KGD's efficacy was observed when animals were maintained on KGD continuously, starting from 10 days prior to the first onset of ABA (i.e., ABA1). Although such observation is promising for future treatments of AN, long-term maintenance on KGD is challenging and can be detrimental physiologically (D'Andrea Meira et al. 2019; Wei et al. 2024). Moreover, it is not likely that individuals would strive to be on KGD prior to the first onset of AN. Thus, in this study, we asked a lingering

TABLE 2 | Group comparison of wheel running of SD➔KGD versus SD➔SD, results of Tukey's multiple comparisons test.

Total running				
Experimental day	**Mean diff**	**95.00% CI of difference**		**Adjusted *p***
ABA1				
Acc4	59.59	−4113 to 4232	ns	0.9769
Acc3	1947	−2446 to 6340	ns	0.3725
Acc2	−3441	−9172 to 2290	ns	0.2302
Acc1	−1794	−9474 to 5886	ns	0.6372
FR1	8118	160.2 to 16,077	*	0.0459
FR2	−387.1	−7864 to 7090	ns	0.9165
FR3	−19,341	−27,719 to −10,962	****	< 0.0001
ABA2				
Acc4	−6954	−11,384 to −2525	**	0.0031
Acc3	−4074	−9127 to 978.8	ns	0.1101
Acc2	−5089	−10,400 to 221.5	ns	0.0597
Acc1	−4468	−11,369 to 2434	ns	0.1963
FR1	6845	210.5 to 13,479	*	0.0436
FR2	10,317	1776 to 18,858	*	0.0196
FR3	7137	−2669 to 16,943	ns	0.1475
FR4	−8429	−16,724 to −134.0	*	0.0466
FAA running				
Experimental day	**Mean diff**	**95.00% CI of difference**		**Adjusted *p***
ABA1				
Acc4	−104.8	−377.5 to 168.0	ns	0.4324
Acc3	85	−41.71 to 211.7	ns	0.1768
Acc2	65.41	−8.107 to 138.9	ns	0.0782
Acc1	1133	427.0 to 1840	**	0.0035
FR1	1123	399.9 to 1847	**	0.0037
FR2	5568	493.3 to 10,642	*	0.0326
FR3	−5380	−11,122 to 361.9	ns	0.0652
ABA2				
Acc4	−577.9	−1815 to 658.7	ns	0.3441
Acc3	43.29	−56.62 to 143.2	ns	0.3749
Acc2	−4.544	−33.76 to 24.68	ns	0.7532
Acc1	19.68	−24.46 to 63.82	ns	0.3653
FR1	18.88	−13.07 to 50.82	ns	0.2328
FR2	4515	798.5 to 8232	*	0.0203
FR3	10,203	3291 to 17,115	**	0.0058
FR4	5689	−114.0 to 11,492	ns	0.0544

(Continues)

TABLE 2 | (Continued)

2 Hr food running				
Experimental day	**Mean diff**	**95.00% CI of difference**		**Adjusted *p***
ABA1				
Acc4	736	−226.9 to 1699	ns	0.1292
Acc3	587.4	−516.1 to 1691	ns	0.2832
Acc2	537.2	−891.3 to 1966	ns	0.4462
Acc1	−136.6	−2045 to 1772	ns	0.8835
FR1	330.6	−934.9 to 1596	ns	0.5977
FR2	−1212	−1964 to −459.3	**	0.0029
FR3	−870.8	−1493 to −248.8	**	0.0081
ABA2				
Acc4	−2880	−4208 to −1553	***	0.0001
Acc3	−2554	−3967 to −1141	***	0.0009
Acc2	−3334	−4990 to −1678	***	0.0003
Acc1	−3513	−5272 to −1754	***	0.0003
FR1	−1395	−3087 to 296.6	ns	0.1024
FR2	−3703	−4828 to −2579	****	< 0.0001
FR3	−3525	−5011 to −2038	***	0.0001
FR4	−3936	−5676 to −2195	***	0.0002
Dark 21–1 running				
Experimental day	**Mean diff**	**95.00% CI of difference**		**Adjusted *p***
ABA1				
Acc4	577.1	−1377 to 2531	ns	0.5504
Acc3	1093	−1606 to 3792	ns	0.415
Acc2	−132.6	−3194 to 2928	ns	0.9301
Acc1	−675.8	−3771 to 2419	ns	0.6593
FR1	−1375	−3908 to 1159	ns	0.2772
FR2	−3637	−7422 to 148.5	ns	0.0591
FR3	−8444	−12,414 to −4474	***	0.0001
ABA2				
Acc4	−2618	−4230 to −1007	**	0.0024
Acc3	−1253	−3614 to 1107	ns	0.287
Acc2	−2447	−5161 to 267.1	ns	0.0753
Acc1	−1620	−4699 to 1460	ns	0.2916
FR1	616	−2553 to 3785	ns	0.6944
FR2	3545	−698.7 to 7790	ns	0.0983
FR3	−1131	−5223 to 2961	ns	0.5769
FR4	−9445	−13,148 to −5742	****	< 0.0001

(Continues)

TABLE 2 | (Continued)

Dark 1–7 running				
Experimental day	**Mean diff**	**95.00% CI of difference**		**Adjusted *p***
ABA1				
Acc4	−1114	−3117 to 888.7	ns	0.2653
Acc3	113.1	−1764 to 1990	ns	0.9026
Acc2	−3955	−6465 to −1445	**	0.0034
Acc1	−2091	−5614 to 1432	ns	0.2351
FR1	5967	2584 to 9349	**	0.0011
FR2	−1138	−4590 to 2314	ns	0.5034
FR3	−2093	−5716 to 1529	ns	0.2478
ABA2				
Acc4	−822.5	−2167 to 522.1	ns	0.2215
Acc3	−314.1	−2479 to 1851	ns	0.7689
Acc2	675.4	−1316 to 2667	ns	0.4933
Acc1	636.3	−3114 to 4387	ns	0.7317
FR1	7170	4113 to 10,228	****	<0.0001
FR2	5368	1954 to 8781	**	0.0034
FR3	1366	−2280 to 5011	ns	0.4506
FR4	−847.9	−3252 to 1556	ns	0.4770

*$p < 0.05$.
**$p < 0.01$.
***$p < 0.001$.
****$p < 0.0001$.

question: Can KGD be introduced *after* ABA1 to ameliorate AN relapses? To answer this question, we investigated the efficacy of treating ABA relapse by shifting animals' diet from standard diet (SD, pellet plus wet food) during ABA1's food-restricted days (FR) to KGD while in recovery from ABA1 and through FR days of ABA2 (Figure 1c). Hence, this experimental group was named the SD➔KGD group. The SD➔KGD group's daily signatures of vulnerability were compared to the SD➔SD group's that were fed SD during ABA1 and ABA2 (Figure 1c, top two rows). Of note, the SD➔KGD group was introduced to KGD, alongside SD during the 5 days of wheel acclimation that preceded the FR days of ABA1. This was to avoid food deprivation due to food neophobia when switching later from SD to KGD, only.

3.1.1 | Wheel Running

ABA vulnerability, quantified based on wheel running, revealed a significant reduction among the SD➔KGD group during ABA2, compared to SD➔SD, when the two groups' diets differed (Table 2). The total wheel count (Total WCT, summed over 24 h of each day, Figure 2a1) during ABA2 of the SD➔SD group increased starting FR1, rose to a higher level by FR2, then declined by the last day of FR, as weight loss became progressively more severe (see Figure 2c). A similar pattern was evident for the SD➔SD group during FAA (the food-anticipatory activity hours that precede the feeding hours, Figures 1b and 2a2) and the dark hours of ABA2 (Table 2). By contrast, WCT of SD➔KGD during ABA2, when they were fed KGD, remained much as they did during the 4 days of acclimation to the wheel without FR (Acc4, 3, 2, and 1), exhibiting a minimal increase of food restriction-evoked increase in wheel running (Figure 2a1,a2).

During ABA1, when both groups were fed SD, wheel running did not differ significantly across the groups (Table 2). SD➔SD's wheel running was as seen during ABA2, rising progressively from FR1 to FR2, then declining on FR3. SD➔KGD's FR-evoked increase in wheel running during ABA1 was delayed by 2 days, possibly reflecting a transient protective effect of KGD during acclimation.

3.1.2 | Food Consumption

ABA vulnerability was quantified, based on severe limitation of food consumption or inability to increase food consumption when returned to ad libitum food. The SD➔KGD group exhibited modestly greater food consumption than the SD➔SD group during FR4 of ABA2 ($p = 0.031$, 12% more) and a significantly greater increase during the recovery phase of ABA2 ($p = 0.0045$, 42% more) (Figure 2b and Table 3). This contrasts with the recovery phase of ABA1, when SD➔KGD were fed KGD, only. This switch in diet caused significant reduction in food consumption, compared to SD➔SD that were fed SD

during this phase ($p < 0.0001$, 31%–49% less, Figure 2b and Table 3). These observations indicate that the dramatic reduction in wheel activity of the SD➔KGD group during FR1-3 of ABA2 is not due to increased caloric intake during those FR days.

3.1.3 | Body Weight

BMI is the strongest predictor of relapse after discharge (Frostad et al. 2022). For young women of average height, weight restoration differing by 5% of baseline can be highly significant, bordering the diagnosis as clinically acceptable (BMI > 18) versus unacceptable (BMI < 17). For mice undergoing ABA, the day-to-day body weight is influenced by food consumption and energy expenditure associated with wheel running. Within any day of FR, body weight would be at its lowest at 7 pm, just prior to feeding, and coinciding with the end of FAA. During ABA2, when the two groups differed in diet, the group difference in weight retention at 7 pm was significant ($p < 0.0001$), with the SD➔KGD group retaining 4 to 5.5% more body weight than the SD➔SD group (Table 4, Figure 2c). During ABA1, SD➔KGD exhibited similarly greater weight retention at 7 pm of FR2 (4%, $p = 0.0005$) and 9 pm of FR2 (4.5%, $p = 0.0027$) than SD➔SD (Figure 2c, Table 4), possibly reflecting residual but transient effects of having been fed KGD together with SD during the preceding acclimation phase.

3.1.4 | EPM

Why does the SD➔KGD group run less than the SD➔SD group? A previous study had shown that wheel running correlates positively with increases in anxiety-like behavior caused by food restriction (Wable, Min, et al. 2015). EPM data support this relationship, since SD➔KGD spent a greater amount of time in the open arms than the SD➔SD group (Figure 2d2), even though the total distance traveled (Figure 2d3) or the frequency of entering the open arms (Figure 2d1) did not differ.

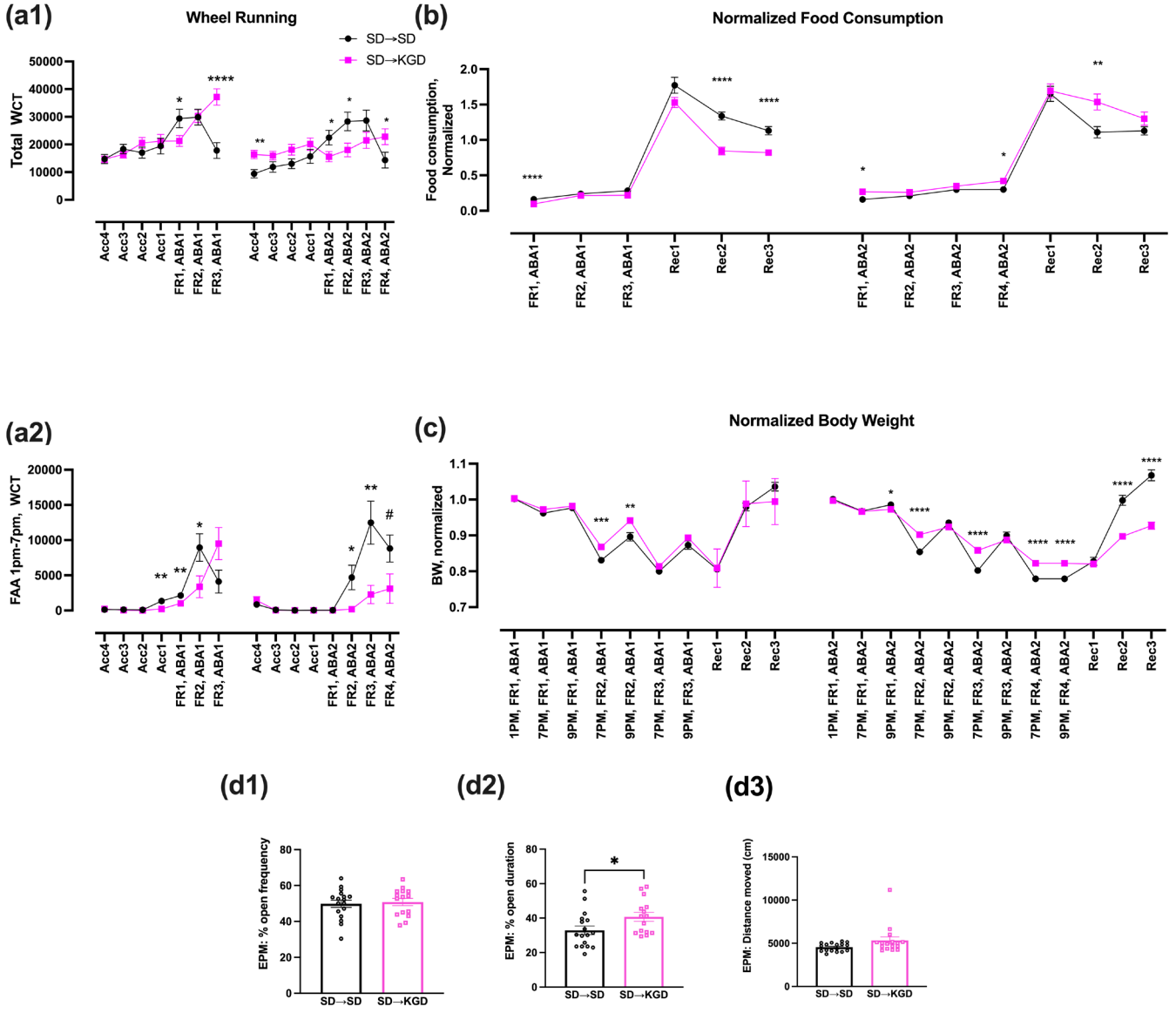

FIGURE 2 | Legend on next page.

FIGURE 2 | KGD treatment that is delayed to ABA2 is still protective against anorexia-like maladaptive behaviors. ABA vulnerability of the SD➔KGD ($N = 17$, pink, square symbols) versus SD➔SD ($N = 17$, black circles) groups, with different diet during ABA2, was compared by quantification of food restriction-evoked hyperactivity on a wheel (panels a1, a2), reduction of food consumption (panel b), and weight loss (panel c) during food restricted days (FR) of ABA1 and ABA2 and anxiety-like behavior on the elevated plus maze (EPM) following recovery from ABA2 (panels d1-d3). The line graphs of *panels a through c* show group means ± SEM (y-axis) of each time point (x-axis). Asterisks indicate significant differences between the two groups at that time point, from Tukey's multiple comparisons tests following repeated measures 2-way ANOVA, allowing for Mixed-effects Model, with diet group and time as the two factors. * indicates $p < 0.05$; ** indicates $p < 0.01$; *** indicates $p < 0.001$; **** indicates $p < 0.0001$. The exact adjusted p values for panels a-c are in Tables 2, 3, and 4. Panel (a1) Wheel counts (WCT) summed over all hours of each experimental day (Total WCT) indicate no group difference prior to FR but a significant increase by FR2 of ABA1, then a decline for the SD➔SD by FR3. By comparison, the SD➔KGD group exhibits a two-day delay in the FR-evoked hyperactivity of ABA1. *This delay may reflect the influence of the* SD➔KGD *group being fed KGD, in addition to SD during the acclimation period*. Unlike the pattern observed during ABA1, during ABA2, after the SD➔KGD group was fed KGD consistently for 10 days, starting from the recovery phase of ABA1, these animals exhibited no FR-evoked increase in hyperactivity, while SD➔SD exhibited FR-evoked hyperactivity, as seen during ABA1. SD➔SD's TOT wheel running was significantly greater than SD➔KGD's on FR1 and FR2. *Panel (a2)* WCT during FAA (Food anticipatory activity, 1–7 pm) of ABA2 indicates that the KGD of the SD➔KGD group during ABA2 is effective in reducing FR-evoked hyperactivity, relative to SD of the SD➔SD group on FR2, FR3, and FR4. *Panel b* food consumption, normalized to the average of 2 days preceding FR, did not differ significantly across the groups during the FR days, except for the last FR day of ABA2, when the SD➔KGD group ate significantly more than the SD➔SD group. The two groups differed significantly during Rec2 and Rec3 following ABA1, when the SD➔KGD were fed KGD. By Rec2 of ABA2, after the SD➔KGD group had been fed KGD diet for 14 days, they consumed significantly more than the SD➔SD group. *Panel c* body weight (BW) of each animal was normalized to its averaged weights on the 2 days preceding FR days of ABA1 and ABA2. On FR days, animals of both groups inevitably lost weight, reflected by their measurements at 7 pm (before food was given for the night) and increased by 9 pm (when food was taken away), and this daily loss accumulated across FR days. The SD➔KGD group lost less weight due to FR on FR2 of ABA1 and all FR days of ABA2, compared to SD➔SD. *Panel d* the bar graphs show comparisons of group means ± SEM (y-axis) from the Elevated Plus Maze (EPM) test measuring anxiety-like behavior. Each point represents the value of one animal. The SD➔KGD group exhibits significantly greater duration in the open field ($p = 0.0370$, $t = 2.183$, $df = 30$, difference between the means 7.813 ± 3.579), while no difference across the groups was detected for the frequency to enter the open field ($p = 0.7286$, $t = 0.3502$, $df = 30$, difference between the means 0.9990 ± 2.852) or the total distance traveled on the maze ($p = 0.0771$, $t = 1.829$, $df = 31$, difference between the means 779.5 ± 426.3 cm).

TABLE 3 | Group comparison of food consumption of SD➔KDG versus SD➔SD results of Tukey's multiple comparisons test.

Experimental day	Mean diff	95.00% CI of difference		Adjusted p
ABA1				
FR1	−0.06742	−0.09658 to −0.03827	****	< 0.0001
FR2	−0.02336	−0.07737 to 0.03064	ns	0.3829
FR3	−0.06393	−0.1299 to 0.002002	ns	0.0568
Rec1	−0.2446	−0.5199 to 0.03066	ns	0.0793
Rec2	−0.4927	−0.6531 to −0.3323	****	< 0.0001
Rec3	−0.3094	−0.4438 to −0.1749	****	< 0.0001
ABA2				
FR1	0.109	0.01649 to 0.2016	*	0.0233
FR2	0.05012	−0.03345 to 0.1337	ns	0.2260
FR3	0.04822	−0.03789 to 0.1343	ns	0.2610
FR4	0.1206	0.01224 to 0.2290	*	0.0305
Rec1	0.04412	−0.2561 to 0.3443	ns	0.7663
Rec2	0.4277	0.1447 to 0.7106	**	0.0045
Rec3	0.1711	−0.05358 to 0.3959	ns	0.1294

*$p < 0.05$.
**$p < 0.01$.
***$p < 0.001$.
****$p < 0.0001$.

3.1.5 | Differences Across the Sexes

Two-way ANOVA, with ABA cycle and sex as the two factors, indicated no difference between males and females in Total wheel running during ABA1, when they were fed SD ($p = 0.806$) or during ABA2, when they were fed KGD ($p = 0.731$) ($N = 16$ for females; $N = 17$ for males). Nor was there any difference across the sexes in wheel running during FAA ($p = 0.850$ for ABA1;

TABLE 4 | Group comparison of body weights of SD➔KGD versus SD➔SD results of Tukey's multiple comparisons test.

Experimental day	Mean diff	95.00% CI of difference		Adjusted *p*
ABA1				
FR1, 1 pm	0.0006763	−0.007029 to 0.008382	ns	0.8589
FR1, 7 pm	0.01044	−0.0008633 to 0.02174	ns	0.0691
FR1, 9 pm	0.005027	−0.01676 to 0.02681	ns	0.6408
FR2, 7 pm	0.0373	0.01756 to 0.05703	***	0.0005
FR2, 9 pm	0.04521	0.01726 to 0.07316	**	0.0027
FR3, 7 pm	0.01387	−0.004092 to 0.03183	ns	0.1253
FR3, 9 pm	0.02044	−0.009490 to 0.05037	ns	0.1735
Rec1	0.003069	−0.1109 to 0.1170	ns	0.9553
Rec2	0.008711	−0.1270 to 0.1444	ns	0.8938
Rec3	−0.04138	−0.1788 to 0.09603	ns	0.5338
ABA2				
FR1, 1 pm	−0.003689	−0.01082 to 0.003441	ns	0.2972
FR1, 7 pm	−0.001407	−0.01541 to 0.01259	ns	0.839
FR1, 9 pm	−0.01246	−0.02440 to −0.0005245	*	0.0413
FR2, 7 pm	0.04761	0.03130 to 0.06391	****	< 0.0001
FR2, 9 pm	−0.01171	−0.02758 to 0.004164	ns	0.1417
FR3, 7 pm	0.05599	0.03958 to 0.07240	****	< 0.0001
FR3, 9 pm	−0.01186	−0.03577 to 0.01205	ns	0.3172
FR4, 7 pm	0.04335	0.02471 to 0.06200	****	< 0.0001
FR4, 9 pm	0.04335	0.02471 to 0.06200	****	< 0.0001
Rec1	−0.00736	−0.03468 to 0.01996	ns	0.5844
Rec2	−0.1008	−0.1337 to −0.06776	****	< 0.0001
Rec3	−0.1406	−0.1777 to −0.1036	****	< 0.0001

*$p < 0.05$.
**$p < 0.01$.
***$p < 0.001$.
****$p < 0.0001$.

$p = 0.342$ for ABA2). Food consumption was not different across the sexes during ABA1 ($p = 0.326$), but approached significance during ABA2, when they were fed KGD ($p = 0.060$, 10% less Kcal consumed by females). Despite this trend towards a difference in food consumption, their normalized weights during FR and recovery did not differ across the sexes for ABA1 ($p = 0.695$ at 7 pm; $p = 0.289$ at 9 pm; $p = 0.117$ during recovery) or ABA2 ($p = 0.306$ at 7 pm; $p = 0.365$ at 9 pm; $p = 0.281$ during recovery). These absences of differences across the sexes indicate that KGD supports reduction of ABA relapse vulnerability of both sexes.

3.2 | KGD'S Ameliorative Effects on ABA Vulnerability Are Not Sustained When Animals Are Returned to Standard Diet but Can Be Sustained When KGD Is Combined With Ketamine Treatment

Staying on KGD long-term would be challenging and possibly also harmful, as KGD continued for more than three weeks can induce senescence (Wei et al. 2024), among other complications (D'Andrea Meira et al. 2019). We have also observed weight loss during non-FR days of some female mice fed KGD (Dong et al. 2024). Thus, we examined whether KGD's benefits are sustained after animals are returned to SD, then re-challenged with ABA. To this end, we followed ABA vulnerability of animals on a diet schedule of SD➔KGD➔SD across the three ABA cycles (Figure 1c), and compared their last two ABA cycles (KGD➔SD, green square data points in Figures 3–6) to the last two ABA cycles of animals maintained on KGD for all three ABA cycles (KGD➔KGD➔KGD, Figure 1c, magenta triangle data points in Figures 3–6). Moreover, case reports on treatments of AN with KGD included sub-anesthetic ketamine (KET) as a component of the treatment and showed remission that lasted for a minimum of 6 months (Calabrese et al. 2022) to multiple years (Scolnick et al. 2020). Inspired by these reports, we asked whether the combination of KGD with KET provides added benefit over KGD alone, by sustaining KGD's benefits. To answer this question, we assessed ABA vulnerability of animals on the schedule of KGD

plus KET during ABA1, followed by SD for one or two ABA cycles (KGD + KET ➔ SD and KGD + KET ➔ SD ➔ SD, Figure 1c, pooled and indicated as KGD + KET ➔ SD, blue round data points in Figures 3–6).

3.2.1 | Wheel Running

During the ABA cycle when all three groups were fed KGD (referred to as "ABA1" for simplicity), there were no significant

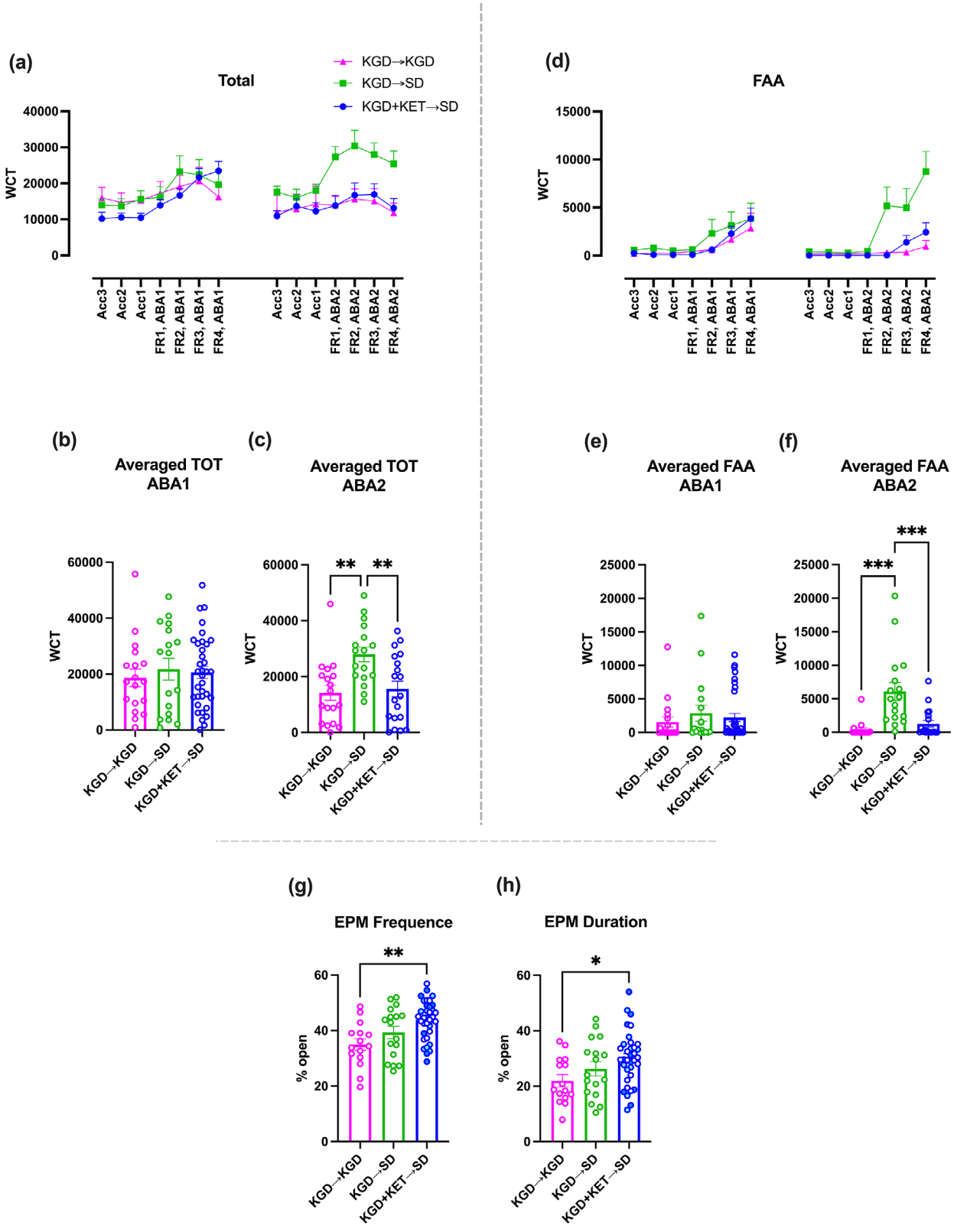

FIGURE 3 | Legend on next page.

FIGURE 3 | Wheel running and anxiety-like behavior of KGD➔SD, KGD➔KGD, and KGD + KET➔SD groups. (a–d) Lines represent day-by-day changes in groups' mean ± SEM daily wheel running, quantified as wheel counts (WCT) across ABA1 and ABA2. Magenta lines with triangle symbols show KGD➔KGD's ($N = 19$), green lines with square symbols show KGD➔SD's ($N = 17$), and blue lines with circles show KGD + KET➔SD's ($N = 35$). For all bar graphs, each animal's WCT, averaged across FR2, FR3, and FR4 or across REC1, REC2, and REC3 of each ABA cycle was calculated and are shown as single data points. The graphs show group mean ± SEM WCT comparisons across the three groups—KGD➔KGD, KGD➔SD and KGD + KET➔SD. (b, c) There is no significant group difference in total (summed for each 24 h period) running during ABA1, but there is a significant group difference during ABA2 ($p = 0.001$, $F(2,51) = 7.544$, One-way ANOVA). Tukey's multiple comparison tests indicate significant differences between KGD➔KGD and KGD➔SD ($p = 0.002$) and between KGD➔SD and KGD + KET➔SD ($p = 0.006$). (e, f) There is no significant group difference in FAA during ABA1, but there is a significant group difference during ABA2 ($p < 0.001$, $F(2,51) = 14.31$, One-way ANOVA). Tukey's multiple comparison tests indicate significant differences between KGD➔KGD and KGD➔SD ($p < 0.001$) and between KGD➔SD and KGD + KET➔SD ($p < 0.001$). (g, h) Elevated plus maze test of anxiety-like behavior. There is a significant group difference in percent frequency to enter an open arm ($p = 0.001$, $F(2, 64) = 7.231$, One-way ANOVA). Tukey's multiple comparison test shows that the KGD + KET➔SD group increased the frequency of entering open arms significantly more than the KGD➔KGD group ($p = 0.001$). There is also a significant group difference in percent duration in entering the open arms ($p = 0.025$, $F(2,64) = 3.905$, One-way ANOVA). Tukey's multiple comparison test shows that the KGD + KET➔SD group increased duration in the open arm more than the KGD➔KGD group ($p = 0.021$).

group differences in total wheel running, summed across 24 h per day of FR (TOT, Figure 3a,b) or FAA (Figure 3d,e). This indicates that KET treatment did not alter wheel running significantly. However, during the FR days of the subsequent ABA (referred to as "ABA2" for simplicity), when their diets and history of drug treatments differed, wheel running also differed across the three groups for TOT (Figure 3c) and FAA (Figure 3f). The KGD➔SD group exhibited significantly greater wheel running compared to KGD➔KGD, indicating that KGD that was fed during ABA1 ceased to suppress the maladaptive FR-evoked hyperactivity for ABA2, after KGD was withdrawn at the end of ABA1. In fact, KGD➔SD's TOT wheel running was similar to that of SD➔SD that were never fed KGD ($p = 0.99$, unpaired t-test, $t = 0.01100$, $df = 30$, $N = 17$ for KGD➔SD, $N = 15$ for SD➔SD, not shown). KGD➔SD's FAA also did not differ from that of SD➔SD ($p = 0.91$, $t = 0.1108$, $df = 35$, $N = 17$ for KGD➔SD, $N = 20$ for SD➔SD, not shown).

KG + KET➔SD group exhibited significantly lower TOT and FAA than KGD➔SD during ABA2 (Figure 3c,f), even though KGD had been withdrawn at the end of ABA1, just as was done for the KGD➔SD. In fact, the suppression of KGD + KET➔SD's TOT and FAA running was as strong as seen for KGD➔KGD's (Figure 3c,f). This pattern during ABA2 for KG + KET➔SD confirmed that KET supplementation of KGD during ABA1 could sustain for 7 to 11 days the suppression of the maladaptive excessive wheel running during ABA2 as effectively as for those kept on KGD through ABA2.

3.2.2 | Anxiety-Like Behavior

Anxiety-like behavior was evaluated using the Elevated Plus Maze (EPM), with the percentage of open-arm entries (Figure 3g) and percentage of the duration spent on the open-arm (Figure 3h) used as indicators of anxiety-like behavior. The KGD + KET➔SD group demonstrated the greatest entries and durations in open arms. These results suggest that KET supplementation not only preserves the anxiolytic and resilience-enhancing effects of KGD in the absence of KGD but may also amplify the anxiolytic effects.

3.2.3 | Food Consumption (FC)

To determine whether dietary composition influenced food consumption, we compared food consumption in KCal (FC) after normalizing to baseline FC (Figure 4). The normalization was performed to remove sex differences in FC that arise from sex differences in body weight. The KGD➔KGD group maintained relatively stable and consistent FC throughout both ABA1 and ABA2 (Figure 4a). Comparisons of the three groups revealed no difference during the FR days of ABA1. This was as expected, since all three groups were fed the same diet of KGD (Figure 4b). KGD➔KGD versus KGD➔SD comparison during the FR periods of ABA2 (Figure 4d) also revealed no significant differences in FC, indicating that KGD did not alter overall food intake. This observation is consistent with earlier observations of comparing FC of SD➔KGD versus SD➔SD (Figure 2b). By contrast, KET that accompanied KGD during ABA1 enhanced the animals' FC during the FR days of ABA2, compared to the FC of those fed KGD without ketamine during ABA1 (KGD + KET➔SD versus KGD➔KGD). This indicates that the addition of KET to the KGD treatment during ABA1 contributed to increases of FC during FR days of ABA2, beyond what could be achieved by KGD alone, sustained for 7–11 days after the last ketamine injection.

During the recovery phase of ABA1 (Figure 4c) and ABA2 (Figure 4e), KGD➔KGD consumed less than both the KGD➔SD and KGD + KET➔SD groups, indicating that KGD has one undesirable effect of delaying weight restoration. This, too, is consistent with what we observed when comparing FC during recovery from ABA2 of KGD➔KGD versus SD➔SD (Dong et al. 2024).

3.2.4 | Body Weight (BW)

Both wheel activity and FC collectively influence BW. Therefore, normalized body weight was tracked across experimental days at time points of 7 pm (beginning of the feeding hours) and 9 pm (end of the feeding hours) on FR days and at 1 pm on non-FR days to evaluate the effects of dietary composition and ketamine treatment on BW regulation (Figure 5). During ABA1, when all three groups consumed KGD, BW did not differ significantly among the three groups at 7 pm or 9 pm of the FR days (Figure 5a–c).

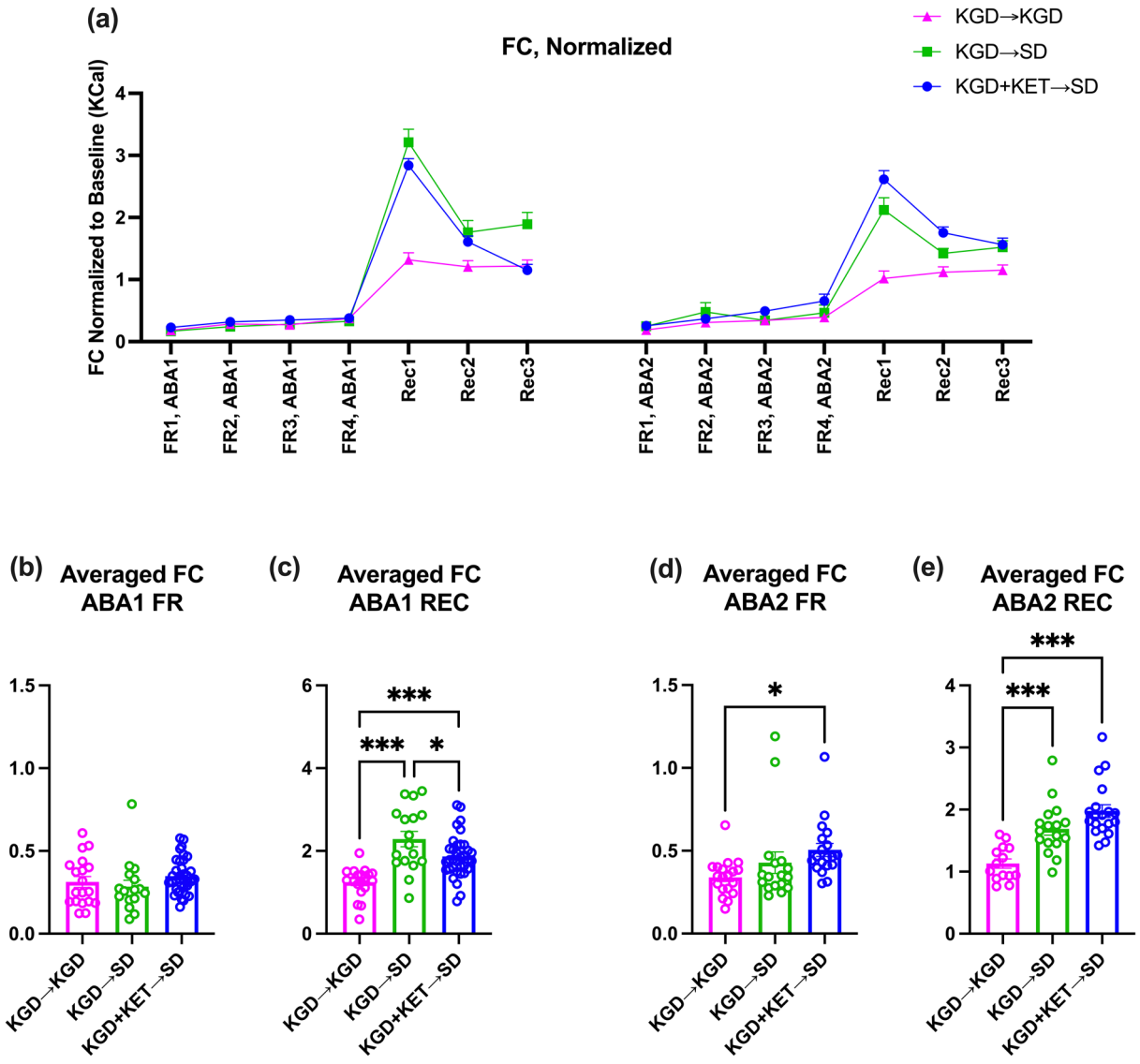

FIGURE 4 | Normalized food consumption of KGD➔SD, KGD➔KD, and KGD + KET➔SD groups. (a) Lines represents day-by-day changes in group mean ± SEM food consumption (FC) in Kcal of the KGD➔KGD (magenta triangles, $N = 19$), KGD➔SD (green squares, $N = 17$) and KGD➔KET➔SD (blue circles, $N = 35$) groups, normalized to baseline FC. For all bar graphs in this figure, each animal's normalized FC, averaged across three FR days or three recovery (REC) days of ABA was calculated and are shown as single data points. The bar graphs show comparisons across the three groups—KGD➔KGD, KGD➔SD and KGD + KET➔SD—of normalized FC (y-axis) against groups (x-axis). Bar = mean ± SEM. (b) There is no significant difference in averaged FC during ABA1 FR period. (c) During the recovery period of ABA1, there is a significant difference in group mean FC ($p < 0.001$, F (2, 68) = 16.35, One-way ANOVA). Tukey's multiple comparison tests indicate significant differences between KGD➔KGD and KGD➔SD ($p < 0.001$), KGD➔KGD and KGD + KET➔SD ($p < 0.001$) and between KGD➔SD and KGD + KET➔SD ($p = 0.031$). (d) There is a significant difference in the group mean FC during ABA2 FR period ($p = 0.036$, F (2, 52) = 3.558, One-way ANOVA). Tukey's multiple comparison tests indicate significant differences between KGD➔KGD and KGD + KET➔SD ($p = 0.027$). (e) During the recovery period of ABA2, there is a significant difference in the group mean FC ($p < 0.001$, F (2, 47) = 18.74, One-way ANOVA). Tukey's multiple comparison tests indicate significant differences between KGD➔KGD and KGD➔SD ($p < 0.001$), and between KGD➔KGD and KGD + KET➔SD ($p < 0.001$).

This indicates that the addition of ketamine to the treatment had no acute effect on BW retention. The three KGD-fed groups' BW differed significantly from the one group that was fed SD: the proportion of animals with BW above 80% during the FR days ("Survival," Figure 6) did not differ among the three KGD-fed groups, while they all differed significantly from those fed SD on FR days of ABA1 ($X^2 = 33.2$, $p < 0.001$ by the Log-rank (Mantel-Cox) survival curve comparison). There was a significant group effect during the recovery period that followed FR of ABA1 (Figure 5d). Tukey's multiple comparisons test revealed that BW was higher in KGD➔SD and KGD + KET➔SD that were fed SD during recovery, compared to KGD➔KGD that were fed KGD during recovery (Figure 5d), with no difference between KGD➔SD and KGD + KET➔SD. This indicates that, in the absence of a wheel and with ad libitum food availability, weight restoration is easier with SD than with KGD. This undesirable property of KGD was observed for the recovery phase of SD➔KGD, compared to SD➔SD (Figure 2b), and in an earlier publication that compared the two diets across 3 cycles of ABA, namely KGD➔KGD➔KGD to SD➔SD➔SD (Dong et al. 2024).

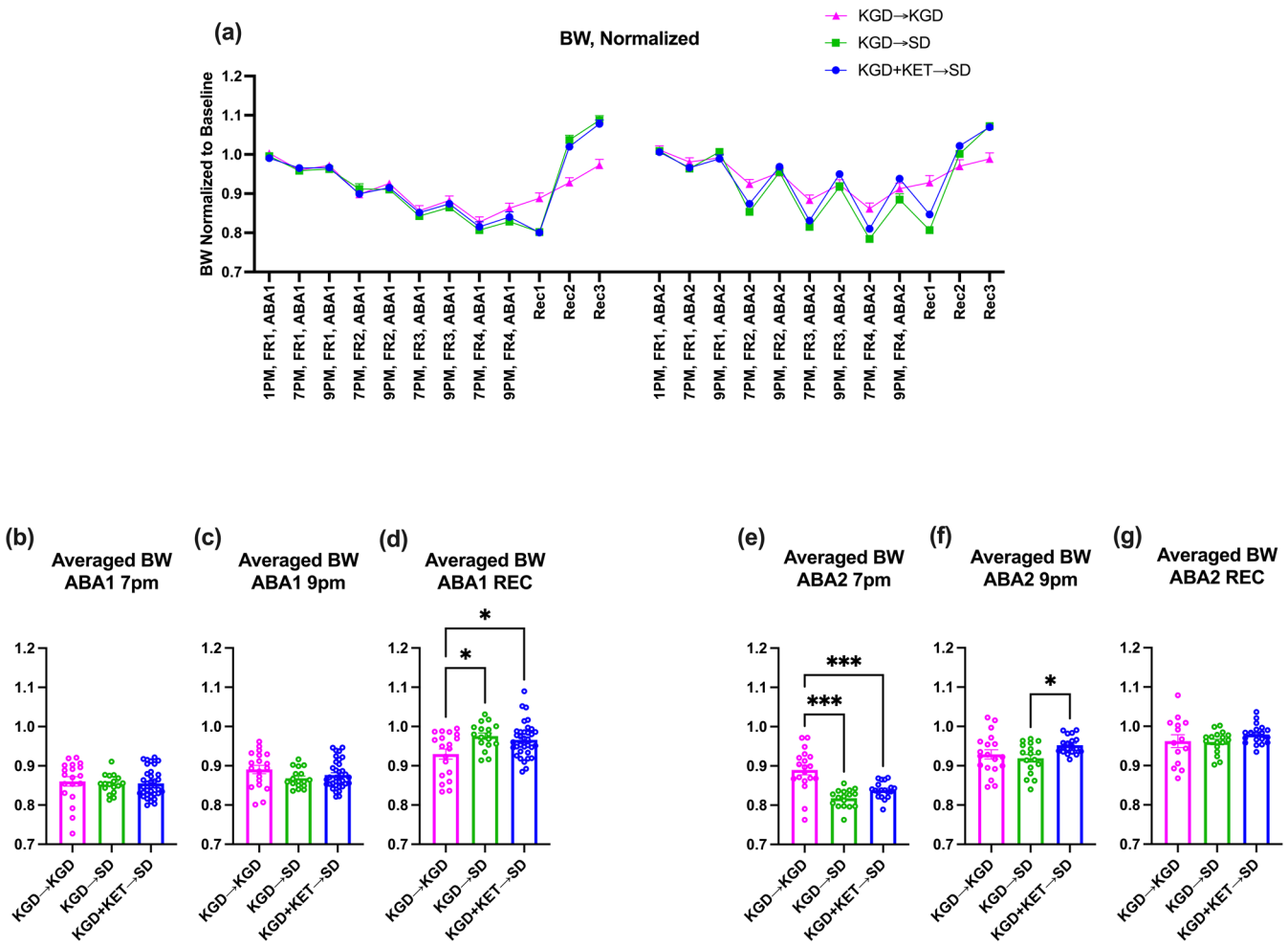

FIGURE 5 | Normalized body weight (BW) of KGD➔SD, KGD➔KGD, and KGD + KET➔SD groups. (a) Lines represent day-by-day changes in group mean values of normalized BW of animals of the KGD➔KGD (magenta triangles, $N = 19$), KGD➔SD (green squares, $N = 17$) and KGD + KET➔SD (blue circles, $N = 35$) groups. The line graph shows KGD➔KGD, KGD➔SD and KGD + KET➔SD's group mean ± SEM of normalized BW (*y*-axis) against each experimental day and time of day (*x*-axis). For all bar graphs in this figure, each animal's normalized BW, averaged across FR2, FR3, and FR4 or across REC1, REC2, and REC3 of ABA was calculated and shown as single data points. The graphs show comparisons across the three groups—KGD➔KGD, KGD➔SD and KGD + KET➔SD—of normalized BW (*y*-axis) against groups (*x*-axis). Bar = mean ± SEM. (b–d) During ABA1 (panels b, c, and d), there is no significant differences in the group mean values at 7 pm and 9 pm, but a significant group mean difference during the recovery period following ABA1, as food transition is occurring ($p = 0.006$, F (2, 68) = 5.479, One-way ANOVA). Tukey's multiple comparison test shows significant differences between KGD➔KGD and KGD➔SD ($p = 0.01$), and between KGD➔KGD and KGD + KET➔SD ($p = 0.017$). BW recovery is favored by SD. (e–g) During ABA2 (panels e, f and g), there are significant group mean differences at 7 pm ($p < 0.001$, F (2, 52) = 19.23) and 9 pm ($p = 0.04$, F (2, 52) = 3.415), but no difference during the recovery period following ABA2. Tukey's multiple comparisons show that, at 7 pm (e), there are significant differences in BW between KGD➔KGD and KGD➔SD ($p < 0.001$) and between KGD➔KGD and KGD + KET➔SD ($p < 0.001$), indicating that KGD is helpful for BW retention. At 9 pm (f), there is a significant difference between KGD➔SD and KGD + KET➔SD ($p = 0.038$), indicating that KET treatment during ABA1 has a sustained benefit.

During ABA2, when the diet and drug treatment history differed, BW differences became pronounced (Figure 5e,f). Of the three groups that had the history of being fed KGD during ABA1, the KGD➔KGD group maintained the most stable BW at 7 pm (Figure 5e). The weight loss for KGD➔SD was as severe as it was for animals that were maintained on SD continuously (81% of baseline weight for both groups, $p = 0.49$, $t = 0.7005$, $df = 32$, $N = 17$ for both groups, not shown graphically). The survival curve comparison, with 80% of baseline BW set as the criterion for survival (Figure 6), yielded similar findings, namely that the SD➔SD and KGD➔SD experienced similar weight loss at 7 pm on FR days of ABA2 (Log-rank (Mantel-Cox) test; $X^2 = 0.72$, $p = 0.40$). Unlike ABA1, the KGD➔SD group experienced the greatest weight loss at both 7 pm (Figure 5e) and 9 pm (Figure 5f) of ABA2, indicating that the protective effects of the KGD diminished after animals returned to SD.

The KGD + KET➔SD group also lost weight significantly at 7 pm of ABA2's FR days, more so than the KGD➔KGD (Figure 5e). However, by 9 pm of the FR phase, the KGD + KET➔SD group demonstrated greater BW compared to the KGD➔SD, reflecting more effective weight gained during the 2-h food access window than the other two groups. Consequently, the "survival" rate did not differ significantly between the KGD + KET➔SD and the

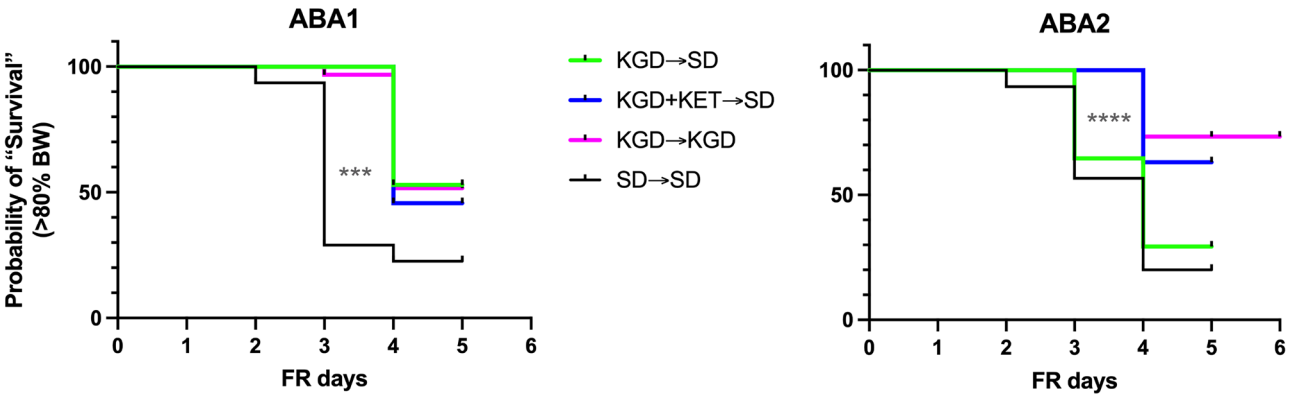

FIGURE 6 | Survival curves of body weights (BW). "Survival," defined as BW at 7 pm on FR days at or above 80% of baseline BW, is plotted for four groups: KGD➔SD ($N=17$), KGD + KET➔SD ($N=35$), KGD➔KGD ($N=31$), and SD➔SD ($N=31$). Asterisks indicate results of curve comparisons, using the Log-rank (Mantel-Cox) test for comparing the four groups simultaneously. For ABA1, Chi square = 33.2, df = 3, $p<0.001$. For ABA2, Chi square = 29.00, df = 3, $p<0.0001$. For ABA1, pairwise comparisons indicate that the SD➔SD group differs from the other three that were fed KGD during ABA1, but the three groups fed KGD do not differ from one another. For ABA2, pairwise comparisons of survival curves indicate that SD➔SD does not differ from KGD➔SD ($p=0.72$). KGD➔KGD does not differ from KGD + KET➔SD ($p=0.46$), either. Results of these survival curve comparisons indicate that (1) the addition of ketamine treatment to short-term KGD is nearly as effective in preventing relapse as is the continuous KGD and (2) returning the diet from KGD to SD causes the return of ABA vulnerability to the level comparable to those that were never treated with KGD.

KGD➔KDG groups during ABA2 (Figure 6, Log-rank (Mantel-Cox) test, $X^2=0.55$, $p=0.46$), while the KGD + KET➔SD's survival curve was significantly different from KGD➔SD'S ($X^2=6.34$, $p=0.01$) and SD➔SD's ($X^2=12.31$, $p=0.0005$), even though they all ate SD during ABA2. These results indicate that ketamine treatment during ABA1 enabled animals to maintain their weights during ABA2 similarly to the animals fed KGD continuously. Moreover, those treated with ketamine regulated their BW significantly better than those fed KGD without ketamine during ABA1. This difference reflect ketamine's sustained action.

In summary, these results suggest that the benefits of the KGD are transient, disappearing upon returning to SD. However, the addition of KET protects from severe weight loss, even without KGD, most likely by promoting increased food consumption during the 2 h of food availability (Figure 4a,d) and also suppressing FR-evoked hyperactivity as effectively as those maintained on KGD (Figure 3c,f). Remarkably, KET's protection was sustained to ABA2, 7–11 days post-injection.

3.2.5 | Comparison of KGD + KET➔SD's Behavior Across the Sexes

Comparison of KGD + KET➔SD's behavior across the sexes (19 females, 16 males) revealed no difference in wheel running during any segment of the day or in food consumption during ABA1 or ABA2 (Table 5). Comparisons across the sexes of normalized body weight revealed no differences during the FR days of ABA1 or ABA2 but revealed significantly greater weight for females during recovery from ABA1 (4.4%, $p=0.002$, Table 5) and no sex differences during recovery from ABA2. Overall, these results indicate that both sexes benefited from receiving KET during KGD treatment for boosting and sustaining resilience against ABA relapses.

3.3 | GABAergic Synapse Plasticity in the PCL of the Dorsal Hippocampal CA1 Correlates With KGD'S Suppression of ABA Vulnerability

We sought to determine whether GABAergic synapse plasticity is enhanced more by KGD than SD following the experience of ABA. To test this hypothesis, we used the approach of electron microscopic immunocytochemistry (EM) to quantify the extent of GABAergic synapses formed onto cell bodies of pyramidal neurons in the pyramidal cell layer (PCL) of the CA1 field of the dorsal hippocampus. Samples were taken from brains of SD➔KGD and SD➔SD females for which behavioral data are shown, after combining with males', in Figure 2 and Results section 3.1. The SD➔KGD ($N=7$) were fed KGD for 19 days that spanned from the recovery days following ABA1 to the end of the recovery days following ABA2, corresponding to the time point of euthanasia. Data from this group will be referred to as "KGD" in Figures 7 and 8. The SD➔SD group ($N=10$) was fed SD for 28 days spanning ABA1 and ABA2, to the point of euthanasia and will be referred to as "SD" in Figures 7 and 8.

Figure 7 shows representative synapses formed by GAD+ (i.e., GABAergic) axon terminals on cell bodies of pyramidal neurons in the pyramidal cell layer (PCL). EM analysis (Figure 7a) revealed that the KGD group displayed significantly longer GAD+ synapse lengths compared to the SD group (Figure 7b). Pyramidal cells of the KGD group also showed a higher proportion of their plasma membrane contacted by GAD+ synapses (Figure 7c), without changes in GABA synapse density (Figure 7d) along the plasma membrane of pyramidal neurons. These results suggest that KGD increased the extent of inhibitory synaptic contact on pyramidal neurons through enlargement of individual synapses, without adding new synapses.

TABLE 5 | Group comparison of the behavior of KGD + KET ➔ SD across the sexes.

ABA1, during KGD + KET treatment				
Source of variation	**% of total variation**	***p***	**Summary**	***F* (*DFn*, *DFd*)**
Averaged wheel running				
Time × sex	0.6745	0.475	ns	$F(5, 165) = 0.9109$
Time	50.59	< 0.001	***	$F(1.44, 47.50) = 68.32$
Sex	0.746	0.3	ns	$F(1, 33) = 1.110$
Tukey's multiple comparisons test	Mean diff. *F* versus *M*	95.00% CI of diff.	Summary	Adjusted *p*
Total	4610	−4217 to 13,437	ns	0.296
FAA	395.5	−2157 to 2948	ns	0.754
2 h FD	364.6	−965.0 to 1694	ns	0.581
Dark 21–1	2499	−1831 to 6829	ns	0.249
Dark 1–7	1197	−2121 to 4515	ns	0.467
Light 7–13	584.8	−644.3 to 1814	ns	0.340
Averaged normalized food consumption				
Source of variation	% of total variation	*p*	Summary	*F* (*DFn*, *DFd*)
Time × sex	0.1083	0.623	ns	$F(1, 33) = 0.2464$
Time	62.55	< 0.001	***	$F(1, 33) = 142.3$
Sex	0.05255	0.78	ns	$F(1, 33) = 0.07927$
Bonferroni's multiple comparison test	Predicted (LS) mean diff.	95.00% CI of diff.	Summary	Adjusted *p*
avg norm FR2,3,4	−0.024	−0.6144 to 0.5655	ns	> 0.999
Recovery avg	0.137	−0.4532 to 0.7267	ns	> 0.999
AVG normalized weights				
Source of variation	% of total variation	*p*	Summary	*F* (*DFn*, *DFd*)
Time × sex	3.825	< 0.001	***	$F(2, 66) = 15.31$
Time	58.4	< 0.001	***	$F(1.054, 34.77) = 233.7$
Sex	0.7049	0.35	ns	$F(1, 33) = 0.8998$
Tukey's multiple comparisons test	Mean diff.	95.00% CI of diff.	Summary	Adjusted *p*
7 pm avg. FR2,3,4	−0.006	−0.03171 to 0.02063	ns	0.667
9 pm avg. FR2,3,4	−0.008	−0.03347 to 0.01782	ns	0.536
Recovery avg	0.044	0.01818 to 0.07060	**	0.002
ABA2, fed SD subsequent to KGD + KET treatment				
Source of variation	**% of total variation**	***p***	**Summary**	***F* (*DFn*, *DFd*)**
Averaged wheel running				
Time × sex	1.146	0.656	ns	$F(5, 85) = 0.6585$
Time	45.85	< 0.001	***	$F(1.248, 21.22) = 26.33$
Sex	0.6748	0.487	ns	$F(1, 17) = 0.5040$

(Continues)

TABLE 5 | (Continued)

ABA2, fed SD subsequent to KGD + KET treatment				
Source of variation	**% of total variation**	***p***	**Summary**	***F* (*DFn*, *DFd*)**
Bonferroni's multiple comparison test	Mean difference	95.00% CI of diff.	Summary	Adjusted *p*
Total	−4191	−23,476 to 15,093	ns	> 0.999
FAA	1142	−1327 to 3611	ns	> 0.999
2 h FD	−527.9	−1597 to 541.1	ns	0.695
Dark 21–1	−1709	−13,084 to 9665	ns	> 0.999
Dark 1–7	−3088	−11,974 to 5798	ns	> 0.999
Light 7–13	−8.385	−65.75 to 48.98	ns	> 0.999
Averaged normalized food consumption				
Time × sex	0.3084	0.465	ns	$F(1, 17) = 0.5590$
Time	73.59	< 0.001	***	$F(1, 17) = 133.4$
Sex	0.5723	0.405	ns	$F(1, 17) = 0.7292$
Bonferroni's multiple comparison test	Mean diff.	95.00% CI of diff.	Summary	Adjusted *p*
avg norm FR2,3,4	−0.046	−0.6659 to 0.5739	ns	> 0.999
Recovery avg	−0.300	−0.9198 to 0.3199	ns	0.529
Averaged normalized weights				
Time × sex	0.2908	0.138	ns	$F(2, 34) = 2.102$
Time	80.39	< 0.001	***	$F(1.749, 29.73) = 581.1$
Sex	0.1579	0.585	ns	$F(1, 17) = 0.3097$
Bonferroni's multiple comparison test	Mean diff.	95.00% CI of diff.	Summary	Adjusted *p*
7 pm avg. FR2,3,4	−0.012	−0.03511 to 0.01080	ns	0.531
9 pm avg. FR2,3,4	−0.009	−0.03852 to 0.02132	ns	> 0.999
Recovery avg	0.005	−0.02874 to 0.03817	ns	> 0.999

*$p < 0.05$.
**$p < 0.01$.
***$p < 0.001$.
****$p < 0.0001$.

The relationship between GAD+ synapses onto pyramidal cell bodies and biometric measurements was examined (Figure 7e–h). For the KGD group, the density of GAD+ synapses correlated significantly ($p = 0.03$) and positively with total wheel activity (sum of running during 24 h), averaged across FR2, FR3 and FR4 of ABA2's FR days. Such a correlation was not observed for the SD group (Figure 7e). This finding suggests that greater inhibitory input to pyramidal neurons may be linked to the increased physical activity that animals exerted during ABA2. Since locomotion is tightly correlated with hippocampal pyramidal neurons' firing (Bland and Oddie 2001; Buzsaki 2002; Li et al. 2012), the positive correlation may reflect correspondingly greater protection against excito-toxicity of pyramidal neurons by enhanced GABAergic inhibition.

Highly significant correlations ($p < 0.01$) were observed between the proportion of pyramidal cell bodies' plasma membrane contacted by GAD+ axon terminals in the PCL of KGD and ABA2 body weight (BW) before FR began (baseline, $p = 0.001$, $R = 0.980$, Figure 7f), 7 pm of FR days ($p = 0.002$), 9 pm of FR days ($p = 0.002$), and during recovery ($p = 0.007$, $R = 0.7969$). No significant associations were observed for the SD group. These correlations with BW suggest that those individuals with the greatest enhancement of GABAergic input to hippocampal pyramidal neurons were the ones that exhibited the best BW retention during ABA2 while on KGD. The strong correlation between BW and GABAergic inhibition that exists prior to ABA2's FR days suggests that the diet may have supported expansion of GABAergic axons during the 9 days of recovery following ABA1, while fed KGD.

A previous study showed that chemogenetic suppression of a subset of hippocampal pyramidal neurons expressing dopamine D2 receptors increases food consumption (Azevedo et al. 2019). Accordingly, enhanced inhibition of these pyramidal neurons by GABAergic axons may also increase feeding. This mechanism may have contributed towards the improved BW retention observed for the KGD group.

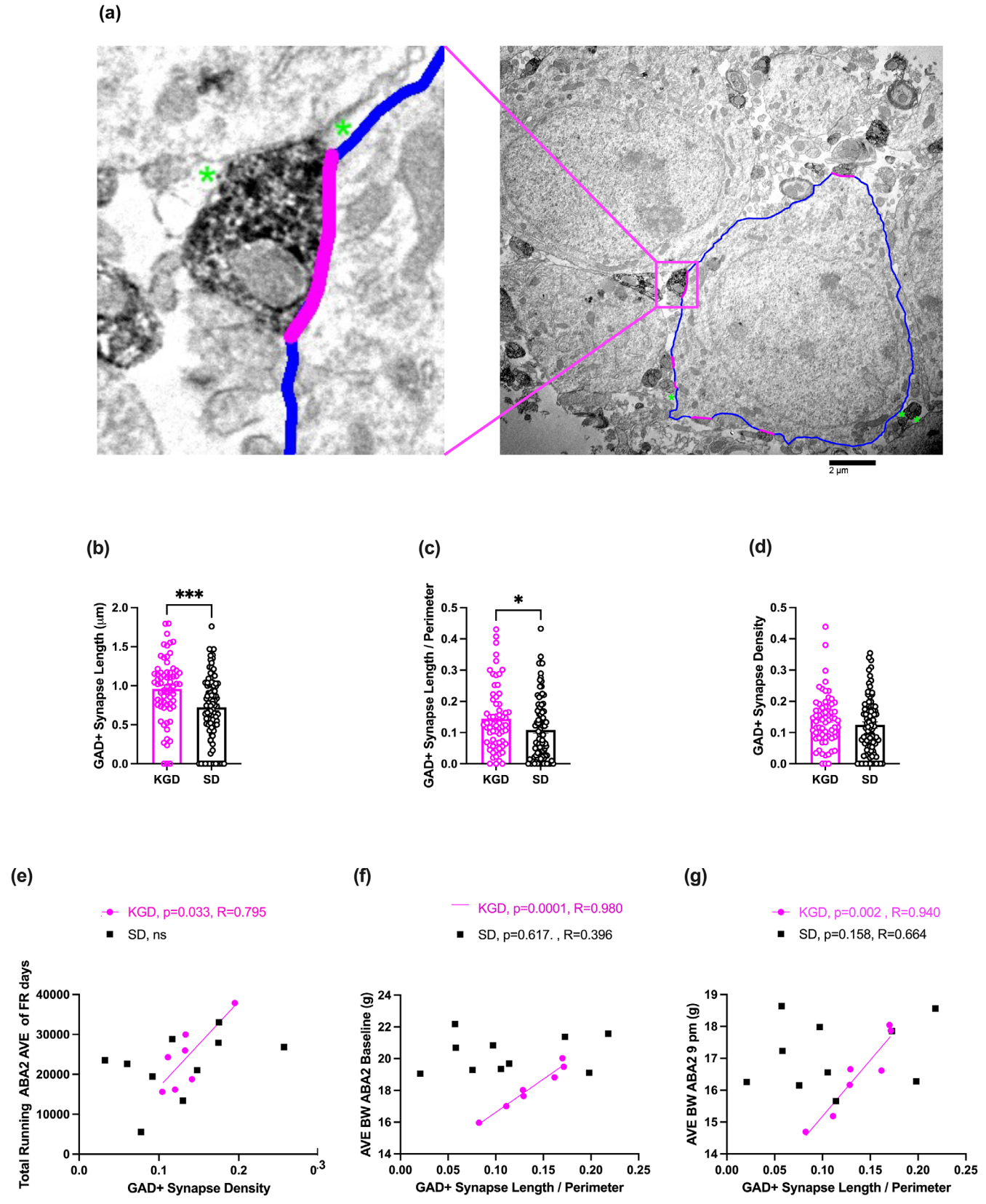

FIGURE 7 | Legend on next page.

FIGURE 7 | Electron microscopic analysis of GAD+ axo-somatic synapses onto pyramidal neurons in the PCL of dorsal CA1 in the KGD versus SD groups. (a) To assess whether the increased ABA resilience accompanying the KGD group could be related to the extent of GABAergic inhibition of hippocampal pyramidal neurons, the ultrastructural pattern of GAD+ GABAergic synapses onto pyramidal neurons was compared across two groups—KGD versus SD. Pyramidal neurons within the pyramidal cell layer (PCL) were identified based on their characteristic round nuclear envelope and the absence of excitatory synapses along their plasma membrane (traced with blue line). For each of the pyramidal cell bodies examined, the lengths of individual GAD+ GABAergic synapses (marked by magenta) and the total plasma membrane (perimeter) of the cell body (indicated by the blue line) were measured. These measurements were used to calculate the proportion of the cell body perimeter contacted by GAD+ axon terminals and the density of GAD+ synapses per cell body perimeter (expressed as the number of GABAergic synapses per 10 mm of perimeter). The average length of GAD+ synapses of each cell body of each animal was also calculated. Asterisks indicate astrocytic processes that form contacts along the sides of GAD+ GABAergic synapses. (b) A comparison of GAD+ GABAergic synapse lengths on each pyramidal neuron between the KGD ($N = 66$ cell bodies) and SD ($N = 95$ cell bodies) groups. The KGD group showed significantly longer lengths compared to the SD group ($p = 0.0006$, $t = 3.502$, $df = 159$). (c) A comparison of the proportion of plasma membrane perimeter contacted by GAD+ GABAergic synapses per pyramidal neuron between the KGD ($N = 66$) and SD ($N = 95$) groups. KGD showed significantly larger proportions of GABAergic contact, compared to the SD ($p = 0.0245$, $t = 2.271$, $df = 159$). (d) There was no significant difference in GAD+ GABAergic synapse density between the KGD ($N = 66$) and SD ($N = 95$) groups. (e) The average value of the density of GAD+ GABAergic synapse along the plasma membrane perimeter was calculated for each animal. Each data point represents the averaged value for one animal. There was a positive correlation between this value and the averaged total running during the FR days of ABA2 for the KGD group (magenta, $p = 0.033$, $R = 0.795$), but not for SD group (black data points). (f–g) Positive correlations existed between each animal's averaged proportion of the plasma membrane perimeter contacted by GAD+ GABAergic synapses and each animal's baseline BW during the 2 days preceding FR of ABA2 ($p = 0.0001$, $R = 0.980$) and at 9 pm of FR days of ABA2 ($p = 0.002$, $R = 0.940$) for the KGD group (magenta circles), but not for the SD group (black squares).

3.4 | GABAergic and Glutamatergic Synapse Plasticity in SLM of the Dorsal Hippocampal CA1 Correlates With KGD'S Suppression of ABA Vulnerability

Unlike the PCL, which is dominated by inhibitory synapses onto pyramidal cells (I-to-E), SLM (stratum lacunosum moleculare) is highly enriched in synapses that are of multiple types: I-to-I synapses formed by inhibitory interneurons onto other inhibitory interneurons that underlie disinhibition; E-to-E at axo-spinous synapses formed between pyramidal neurons, using glutamate as the neurotransmitter; E-to-I formed by excitatory axon terminals of pyramidal cells onto dendritic shafts of GAD+ dendrites, driving inhibition; and I-to-E, formed by GAD+ axons onto dendrites of pyramidal neurons, contributing to the suppression of excitability of the neuropil. Examples of these four synapse types in SLM are shown in Figure 8a,b. We quantified the prevalence of these four synapses within SLM. Group comparison across the KGD and SD revealed no difference in prevalence for any of the four types of synapses (Figure S1), except for the E-to-I. For this E-to-I type of synapse, there was a significantly greater proportion of GABAergic dendrites forming E-to-I for the KGD ($p < 0.005$, $t = 2.948$, $df = 38$, $N = 19$ for SD, 21 for KGD) (Figure 8g).

We estimated the strength of the synapses, based on synapse lengths. The analysis revealed no group difference in the areal density, lengths, or proportion of GABAergic axons forming I-to-E or I-to-I synapses (Figure S1). No difference in GABAergic synapse lengths was detected, although it trended towards significance, with a 10% reduction in the KGD group ($p = 0.053$, $N = 489$ for KGD, $N = 493$ for SD).

To assess the functional significance of the four synapse types to behavior elicited by ABA, we ran Pearson correlation analyses. This analysis revealed that the strengths of correlation between the prevalence (density or proportion) of specific synapse types and behavior differed across the two diet groups.

I-to-I synapses correlated with FAA of both the SD and KGD groups, but oppositely. The SD group trended towards a positive correlation between FAA on FR days of ABA2 with the proportion of GABAergic axons engaged in I-to-I synapses (Figure 8c). I-to-I disinhibition potentially heightens the excitability of pyramidal cells that are postsynaptic to GABAergic neurons engaged in disinhibition. This relationship between neuropil excitability and heightened FAA agrees with our previous findings of animals fed SD (Chowdhury et al. 2013). By contrast, animals fed KGD exhibited a highly significant correlation that was negative, in relation to the prevalence of I-to-I synapses. FAA was greatly reduced overall for the KGD group (Figure 2a2, also note the y-axis values of Figure 8c) and those that exhibited nearly zero FAA were the ones with the greatest proportion of GABAergic axons engaged in I-to-I synapses (Figure 8c). One possible explanation for this highly contrasting correlation across diet groups is that switching of the diet caused switching in the circuits involving I-to-I synapses. For both the SD and KGD groups, the presynaptic GABAergic neurons engaged in I-to-I synapses are likely to be VIP+ GABAergic interneurons (Kepecs and Fishell 2014). However, GABAergic interneurons that receive GABAergic inhibition can be the Parvalbumin+ (PV+) or somatostatin+ (SSt+) types, the latter of which occur as numerous subtypes (Kepecs and Fishell 2014). Perhaps GABAergic axons of the SD group target a different sub-population of GABAergic interneurons than those on the KGD diet. Prior studies have shown that excessive wheel running of ABA animals stem from heightened anxiety (Wable, Min, et al. 2015) and that the hippocampus is an important brain region for anxiety regulation as well as learning (Shen et al. 2010). Based on the positive correlation observed for the SD group, their postsynaptic GABA neurons may be directly involved in disinhibiting pyramidal neurons that drive anxiety-evoked hyperactivity. By contrast, the postsynaptic GABA neurons of the I-to-I synapses of the KGD group may target pyramidal cells that are more actively engaged in the other important hippocampal function—cognition. Food and wheel running are both

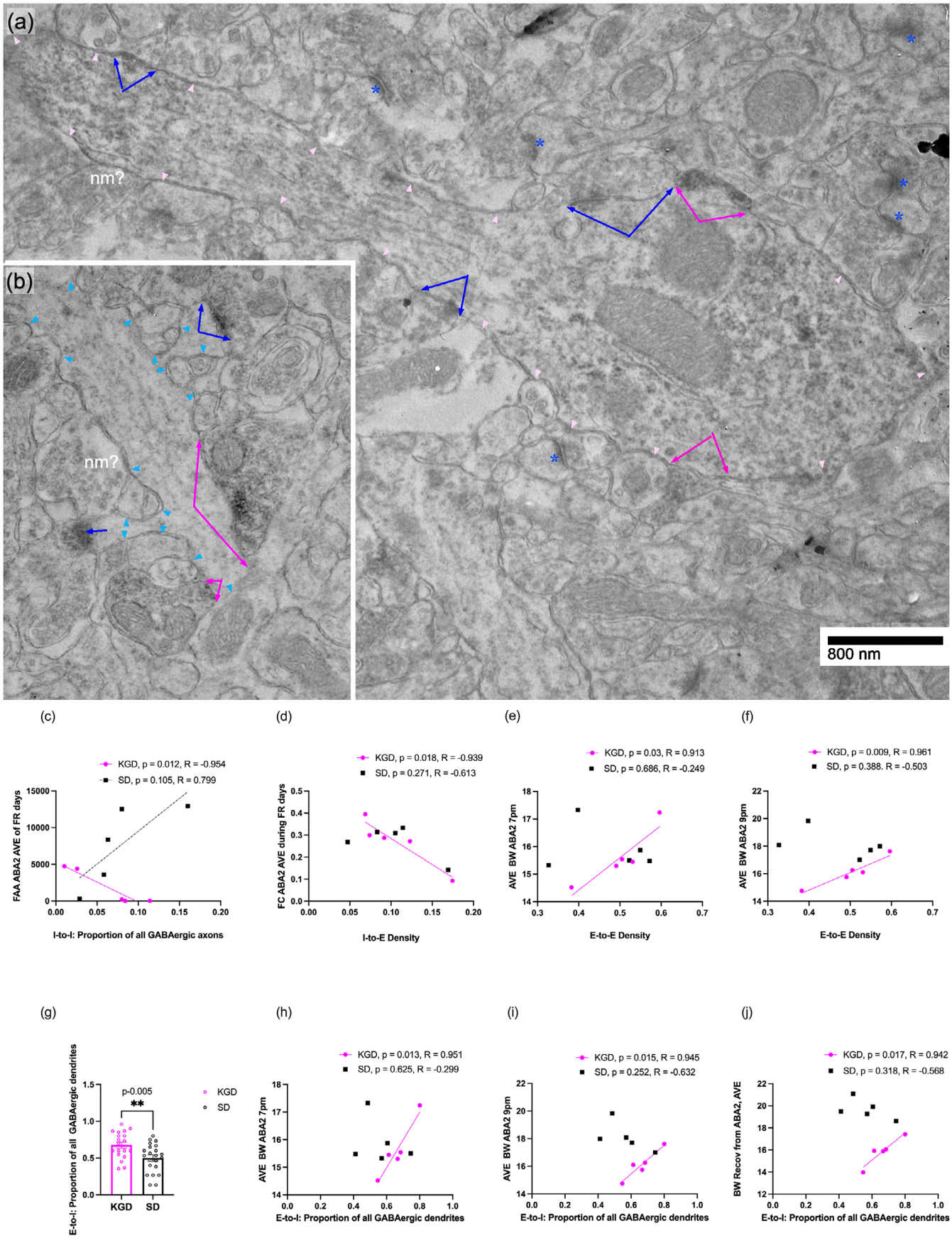

FIGURE 8 | Legend on next page.

FIGURE 8 | EM analysis of axo-dendritic synapses in stratum lacunosum-moleculare (SLM). (a) GAD-immunopositivity of the dendrite is indicated by the accumulation of diffuse, electron-dense HRP/DAB labels along the intracellular surface of the dendrite's plasma membrane and intracellularly. The GAD+ plasma membrane is highlighted by small light pink arrowheads. The larger blue arrows point to excitatory synapses formed onto this GAD+ dendrite, indicated by the thick post-synaptic density (PSD) along the intracellular surface. These E-to-I contacts reflect excitation of the inhibitory neuron, contributing to strengthening inhibition. The dark pink arrows (two pairs) point to inhibitory synapses formed by GAD+ axon terminals. GAD positivity of the axon terminal is indicated by the accumulation of HRP/DAB labels that fill the cytoplasm of the axonal cytoplasm but are excluded from vesicles' lumen (I-to-I). These I-to-I reflect inhibition of an inhibitory neuron, or disinhibition. (b) Synapses onto a dendrite lacking GAD-immunoreactivity, indicating that it belongings a pyramidal neuron. Plasma membrane is highlighted by small light blue arrowheads. The pyramidal neuron's dendrite exhibits excitatory synapses at the tip of two spines, highlighted with dark blue arrows. This reflects excitation of an excitatory neuron (E-to-E). Blue asterisks in panels (a) and (b) highlight additional E-to-E excitatory synapses in the surrounding neuropil formed onto dendritic spines of pyramidal neurons. The pyramidal neuron's dendrite exhibits two GAD+ synaptic inputs onto the dendritic shaft, depicted with dark pink arrows and reflecting inhibition of an excitatory neuron (I-to-E). Both panels show contacts of vesicle-filled axon terminals onto dendritic shafts. There are axon terminals filled with vesicles, lacking GAD-immunoreactivity or association with thick PSDs. These, highlighted as "nm?," may be GABAergic axon terminals with low abundance of GAD or terminals releasing neuromodulators. Both figures were acquired from a brain of a KGD group. (c–h) Quantitative analyses of synapse types in the SLM and their relations to biometrics. In all panels except for (g), each data point represents the averaged value of one animal. For panel (g), each point represents the average value from 5 electron micrographs, representing 210 μm^2 of SLM neuropil, with multiple points derived from one animal. (c) I-to-I synapses: The proportion of all GAD+ axons in KGD brains forming synapses onto GAD+ dendrites correlated negatively with FAA during the FR days of ABA2. KGD animals with higher proportion of their GABAergic axons forming I-to-I synapses exhibited the lowest FAA. SD group showed a trend towards positive correlation. FAA is wheel running during the hours of 1 pm to 7 pm, when animals are the most deprived of food. FAA values of the 2nd, 3rd and 4th days of FR of ABA2 were averaged (AVE). (d) I-to-E synapses: The areal density of inhibitory synapses on unlabeled (presumably pyramidal neurons') dendrites in the SLM neuropil of KGD brains correlated negatively with food consumption (FC) averaged across the 2nd, 3rd and 4th FR days of ABA2. Such a correlation was absent for the SD. (e and f) E-to-E synapses: The areal density of axo-spinous synapses formed by glutamatergic axon terminals onto pyramidal neurons correlated with BW of the KGD animals at 7 pm, when their weights were the lowest, and at 9 pm, just after feeding, when their weights were the greatest within the 24 h of FR. The weights were not normalized to baseline but were averaged across FR2, 3 and 4. Such correlations were absent from the SD group. (g) E-to-I synapses: The proportion of all GABAergic dendrites receiving excitatory input was significantly greater for the KGD than SD ($p < 0.005$, $t = 2.948$, df = 38, $N = 19$ for SD, 21 for KGD). (h–j) E-to-I synapses: The proportion of all GABAergic dendrites receiving excitatory input correlated significantly and positively with KGD group's averaged BW at 7 pm and 9 pm of ABA2 as well as the recover days from ABA2. Such correlations were absent for the SD group.

naturally appetitive, but for ABA animals, those that exhibit ABA resilience choose to eat and suppress wheel running. If KGD supports switching of circuits, the switching could be at the level of GABAergic interneurons or the population of pyramidal neurons subserving the diverse functions of the hippocampus.

E-to-I synapses contributed significantly to BW regulation of the KGD group but not the SD group. The density of these synapses correlated positively with the extent of body weight (BW) gained during ABA2 and the recovery phase following ABA2 (Figure 8h–j). E-to-I synapses were identified by the presence of thick postsynaptic density along the intracellular surface of plasma membranes (PSD) of dendrites immune-positive for GAD (Figure 8a, blue arrows). Through an increase in number (Figure 8g) and synapse strength, KGD may have supported greater excitatory synaptic drive onto GABAergic dendrites in SLM, thereby boosting GABA tone that contributes to anxiolysis. Like the boosting of GABA tone in the PCL through augmented GABAergic innervation of pyramidal neurons' cell bodies, anxiolysis generated through augmented E-to-I synapses onto pyramidal neurons' dendrites in the SLM could have helped animals retain and restore BW better by promoting them to run less and choose to eat, together yielding better weight restoration.

The prevalence of *E-to-E synapses*, formed among pyramidal neurons in the SLM, correlated tightly with BW regulation of KGD but not of SD group. The correlation for the KGD group was strong during ABA2, both at 7 pm, when animals are challenged to retain their weight in the absence of food by suppressing wheel running, and at 9 pm, when animals' weights reflected their ability to choose to eat, rather than run, during the limited hours of food availability (Figure 8e,f). This relationship between E-to-E synapses and BW regulation was somewhat contrary to expectation, in face of the observation that enhanced inhibition of cell bodies of pyramidal neurons in the PCL (Figure 7f,g) and enhanced excitatory drive of inhibitory neurons through E-to-I (described in the paragraph above) also improves BW regulation.

Hippocampus serves a dual role: anxiety regulation and cognition (Shen et al. 2010). It is possible that the two neurotransmitter systems (GABA and glutamate) collaborate in BW regulation by reducing anxiety (through GABA tone boosts) and enhancing cognition (through glutamatergic excitatory synaptic plasticity) Remarkably, both correlations emerged for the KGD-fed animals but not for those kept on SD, even though the areal density of the axo-spinous synapses did not differ across the two groups. The strengthened participation in BW regulation without changes in the density of E-to-E axo-spinous synapses suggests that KGD may strengthen the participation of E-to-E synapses for cognitive function through increased expression of glutamatergic receptors at the E-to-E synapses. KGD promotes BDNF synthesis (Sleiman et al. 2016) and BDNF is a key molecule promoting glutamatergic synapse strengthening (Korte et al. 1998) as well as GABA synaptogenesis (Jiao et al. 2011; Marty et al. 1996).

As for the *I-to-E synapses* in the SLM, their prevalence in brains of the KGD group correlated negatively with food consumption (FC) (Figure 8d), while the SD group exhibited no such correlation. This was contrary to expectation, based on a prior study indicating that chemogenetic inhibition of dopamine D2R-expressing pyramidal neurons in the hippocampus promotes feeding (Azevedo et al. 2019). For the ABA animals fed KGD, GABAergic axon terminals may target the complementary non-D2R pyramidal neurons. Alternatively or in addition, for the KGD group, inhibitory axons targeting pyramidal neurons could also diverge and also be part of the I-to-I disinhibitory circuit that enhances the excitability of the D2R+ pyramidal neurons, thereby exciting the D2R+ pyramidal neurons that lead to suppression of FC (Azevedo et al. 2019).

4 | Discussion

We investigated the therapeutic potential of KGD in mitigating the vulnerability of adult mice to ABA relapses, a well-validated preclinical model of AN (Aoki 2020; Klenotich and Dulawa 2012). The rationale for focusing on ABA relapses in adulthood stems from the fact that individuals who continue to experience AN into adulthood face higher risks of relapses compared to those who recover during adolescence (Berends et al. 2018; McFarlane et al. 2008; Walsh 2013). Our earlier ABA studies align with the age-dependent relapse rates noted for patients diagnosed with AN. Half of the mice that undergo ABA induction in mid-adolescence exhibit a gain of resilience during recovery, even in the absence of pharmacotherapeutic aids, making them more resilient when challenged with a second ABA induction. Those that have gained resilience to a re-challenge of ABA in late adolescence exhibit enhanced GABA synaptic innervation of pyramidal cell bodies and dendrites in the hippocampus, indicating a link between GABA synapse plasticity, reduced excitability of hippocampal pyramidal neurons, and ABA resilience. By contrast, animals that undergo ABA induction in late adolescence rarely gain resilience when re-challenged with ABA induction in adulthood (Aoki and Santiago 2022). Noting this age-dependent difference in the gain of resilience, this study aimed to find treatments that could promote the gain of resilience, especially in adult ABA mice. Results of this study show that 10 days of KGD could reduce ABA susceptibility of adults during ABA2, even after having undergone severe ABA1 while fed SD. Moreover, we learned that KGD enhances synaptic plasticity in the hippocampus, potentially reducing anxiety through GABAergic boosts and stronger excitatory drives of GABAergic neurons. KGD also strengthened the glutamatergic pathway's contribution to body weight retention, indicating that both GABAergic and glutamatergic synaptic plasticity are at play under KGD's influence during ABA. However, the gain of ABA resilience under KGD was not sustained when animals were returned to SD. This finding suggests that KGD may be advisable for patients who have experienced the first onset of AN: KGD may ameliorate or even prevent relapses. However, KGD alone may not be able to instill plasticity once the diet is discontinued. The combination of KGD and KET reduced ABA vulnerability even after KGD was withdrawn. These findings suggest that the resilience associated with ongoing KGD can be replaced with a shorter KGD intervention when paired with KET.

4.1 | The Transience of KGD'S Benefit and Its Relation to the Transience of Ketone Bodies' Effects

KGD's transience may be expected, based on KGD's direct effect, which is to increase fat deposits in the body (Kinzig et al. 2010). Such a change in body composition could reduce animals' experience of hunger when food restriction is imposed, thereby reducing anxiety and the anxiety-evoked propensity to run excessively on the wheel, consequently minimizing weight loss (Wable, Min, et al. 2015). An even more direct consequence of KGD is the elevation of ketone bodies, namely beta-hydroxybutyrate (BHB), which pass the blood-brain barrier and reduces excitability of neurons (Hartman et al. 2007) through direct and immediate alteration of mitochondrial permeability transition (Kim et al. 2015). Lowered blood glucose, which accompanies KGD, also reduces neuronal excitability. In support of the importance of the lowered glucose effect in reducing neuronal excitability, the anti-convulsant effect of KGD is reversed within 2 h of glucose infusion, which also reduces BHB in the same time frame (Huttenlocher 1976). The rapid decline of ketone bodies following the rise of blood glucose level, coupled with the short half-life of ketone bodies (5 h, due to urinary clearance and metabolism by oxidative phosphorylation), explains why KGD's effects on ABA vulnerability could dissipate rapidly after discontinuation of KGD.

However, BHB is also a signaling molecule, operating as an endogenous histone deacetylase inhibitor that favors the expression of multiple genes, including the *BDNF* gene (Sleiman et al. 2016). BDNF fosters glutamatergic (Danzer and McNamara 2004; Korte et al. 1998; Panja and Bramham 2014) and GABAergic (Jiao et al. 2011; Marty et al. 1996) synaptic plasticity. Indeed, our current EM analysis demonstrated for the first time that KGD (from the SD➔KGD group) promotes GABAergic synaptic inhibition of hippocampal pyramidal neurons' cell bodies through lengthening of individual GABAergic axon terminals. This KGD influence, together with the increased prevalence of E-to-I synapses in SLM, is likely to have contributed to improved body weight regulation of animals undergoing ABA. Earlier studies did not detect the augmentation of GABA levels in mouse forebrain, mouse cerebellum, mouse or rat whole brain, or mouse neocortex (reviewed in Hartman et al. (2007)). The discrepancy between our findings and others' may be due to a selective augmentation of GABAergic synapses in the region that we analyzed or due to changes in synaptic structure (which we analyzed), not GABA levels that other labs analyzed.

Our current EM analysis did not detect changes in lengths or density of glutamatergic synapses by KGD. However, the prevalence of glutamatergic synapses in SLM correlated significantly with improvements in body weight retention for the KGD group. Even without structural changes, enhanced BDNF activity resulting from KGD may have contributed towards strengthening of glutamatergic synapses through up-regulation of AMPA-type glutamatergic receptor expression, thereby enhancing glutamatergic synapses' contribution to behavior. Such a BDNF effect of AMPA receptor up-regulation has been documented in studies examining BDNF's mechanism of action as an anti-depressant (Fukumoto et al. 2020; Krystal et al. 2024).

4.2 | KGD'S Protection Against Inflammation

Patients diagnosed with AN are reported to suffer from augmented stress sensitivity (Schmalbach et al. 2020) and to also suffer from low-grade systemic inflammation, characterized by microglial activation and elevation of pro-inflammatory cytokines (e.g., IL-1β, TNF-α) (Pisetsky et al. 2014).

These changes disturb the bi-directional gut-brain system (Belmonte et al. 2016), causing neuroinflammation and neurodegeneration in brains of anorexia-model rats (Reyes-Ortega et al. 2020). KGD may have augmented ABA resilience by reducing pro-inflammatory cytokines via TLR4/NF-κB pathway inhibition (Dilimulati et al. 2023; Polito et al. 2023). The positive correlation between the density of E-to-E synapses in the SLM and body weight retention during the FR days of KGD's ABA2 suggests that KGD may have reduced synapse weakening accompanying neuroinflammation, thereby improving hippocampus-based cognitive abilities (Attaallah et al. 2024; Sosa and Giocomo 2021), such as the decision to navigate towards food rather than to run on a wheel due to anxiety, leading to better body weight retention.

KGD boosts mitochondria biogenesis (Bough et al. 2006), which leads to an increase in ATP production. Enhancement of ATP production as well as of ketone bodies under the condition of KGD augments K_{ATP} channel activity of excitable cells, including hippocampal neurons (Tanner et al. 2011), serving to reduce epileptic seizures of seizure-prone brains. Such augmentation of K_{ATP} channel activity may have worked in concert with GABAergic synaptic inhibition to suppress the excitability of the hippocampus of ABA brains. We surmised that such structural changes to mitochondria and synapses might have been sustained even after KGD withdrawal. Unfortunately, these structural changes, if applicable to ABA, did not sustain behavioral amelioration without ketamine.

4.3 | Sub-Anesthetic Ketamine as an Adjunctive Therapy for Short-Term KGD

While KGD has efficacy in reducing ABA's maladaptive behaviors, long-term adherence to KGD may pose several risks. Chronic use of KGD has been associated with adverse metabolic effects, including dyslipidemia, characterized by elevated levels of low-density lipoprotein (LDL) and total cholesterol, which may increase cardiovascular risk over time (Liu et al. 2018). Nutritional deficiencies are another concern, as the restrictive nature of the diet can lead to inadequate intake of essential vitamins and minerals, such as vitamin D, calcium, and selenium, necessitating ongoing supplementation (Kossoff et al. 2018). Gastrointestinal issues, such as constipation, diarrhea, and abdominal pain, are common and may persist with prolonged use. Long-term KGD use may also impact bone health, with studies suggesting reduced bone mineral density (Bergqvist et al. 2005). Cellular senescence is yet another potential complication accompanying long-term KGD (Wei et al. 2024). These risks underscore the importance of regular monitoring and individualized management to mitigate potential harms while maintaining therapeutic benefits. Within the context of AN treatment, we noted previously (Dong et al. 2024) and in this study (Figure 2b,c) that long-term maintenance on KGD has the drawback of delaying weight restoration of ABA animals in recovery. A welcomed finding of this study is that co-administration of KET with KGD prolongs KGD's protective effects for 28 days (two subsequent cycles of ABA), minimizing ABA vulnerability during relapses, even after cessation of KGD. During ABA2, the KGD + KET ➔ SD group, which went off of KGD, consumed food significantly more than those that continued on KGD (KGD ➔ KGD). During recovery from ABA2, the KGD + KET ➔ SD also consumed food significantly more than those recovering on KGD ➔ KGD. These findings provide hope that KGD can be curtailed to become short-term when accompanied by sub-anesthetic KET. This shift of KGD's transient effect to becoming prolonged may arise from KET's ability to enhance neuroplasticity (described below), complementing KGD's metabolic, structural, and synaptic plasticity-promoting actions described above.

Ketamine, alone, has been shown to reduce maladaptive behaviors in ABA by enhancing glutamatergic synaptic plasticity in the prefrontal cortex (Li et al. 2024; Temizer et al. 2023) and GABAergic synaptic plasticity in the PCL of the hippocampus (Dong et al. 2025). The prefrontal cortex and hippocampus are two regions critically involved in anxiety regulation, cognitive flexibility, and decision making—to eat or to run (Aoki and Santiago 2022). Insights into the molecular mechanisms underlying sub-anesthetic ketamine's action in the brain have progressed mostly from animal models of stress-induced depression. Ketamine is a dissociative anesthetic and non-competitive open-channel blocker of NMDA receptors. At a sub-anesthetic dose, ketamine is hypothesized to selectively target overly active synaptic pathways underlying maladaptive behavior and thoughts (Kim et al. 2023; Li et al. 2024; Temizer et al. 2023). As for sub-anesthetic ketamine's *sustained* action as an antidepressant, it evokes de novo synthesis of multiple synaptic proteins, in addition to BDNF, through de-suppression of local (synapse-specific) protein synthesis. BDNF signaling leads to the phosphorylation of MeCP2 which, in turn, regulates transcription of multiple genes (Kim et al. 2023). This multi-step change in gene transcription, signaling pathways, plus recruitment of the CaMKII-dependent calcium signaling (known to be auto-sustained) is theorized to converge, producing ketamine's prolonged antidepressant effects.

Ketamine's sustained effects as an antidepressant are well-recognized, but most of the in vivo and in vitro assays using animal models were conducted within a day or a week after ketamine administration. By contrast, the KGD + KET ➔ SD ABA animals of this study were shown to exhibit the sustained benefit of ketamine for much longer—14–28 days. The combined KGD + KET treatment may evoke plasticity in ways that are similar to the above-described steps for antidepression but amplified, through initiation of signaling pathways arising separately from ketamine and KGD and converging to up-regulate BDNF synthesis. Conversely, the reason KGD, alone, could not sustain ABA resilience in the absence of ketamine may be because GABAergic synapses withdrew in the absence of ketamine or KGD. This theory can be tested in the future by comparing GABAergic synapses in the hippocampus of KGD ➔ SD versus KGD + KET ➔ SD animals.

4.4 | Future Directions

Other than using ketamine to prolong KGD's benefit, intermittent KGD cycles or exogenous ketone supplementation may help maintain KGD's effects. Biomarkers, such as baseline TLR4 activity and assessment of GABA levels within discrete brain regions, including the hippocampus, may help to personalize treatments of AN relapses. Our study focused primarily on hippocampal mechanisms, leaving unexplored other pathways critically involved in habit formation and anxiety regulation, such as the cortico-striatal circuits and amygdala-based fear networks. Studies are underway to examine how KGD, with and without ketamine, modulates these systems for gaining a more comprehensive understanding of their therapeutic action.

4.5 | Translational Implications

Two earlier case studies that inspired this preclinical study reported that ketamine, combined with KGD, is a recommendable treatment for AN relapse (Calabrese et al. 2022; Scolnick et al. 2020). The case studies reported on six patients, all outpatient females but with severe and enduring AN. This preclinical study analyzed 71 adult mice, building on two prior studies that analyzed the efficacy of KGD alone ($N = 25$) (Dong et al. 2024) and ketamine alone ($N = 14$) (Dong et al. 2025). Results of the current study are robust, revealing significant differences in ABA vulnerability among the groups on KGD versus SD versus KGD + KET. Given the challenges of dietary adherence in individuals with AN, the combinatorial approach of KGD + KET may offer a more feasible strategy for reducing relapse risks. While further studies are needed to determine underlying mechanisms and clinical applicability, these results indicate that brief metabolic and pharmacological interventions synergize to enhance long-term behavioral stability.

Data Availability Statement

The data that support the findings of this study are available from the corresponding author upon reasonable request.

References

Aoki, C. 2020. "Activity-Based Anorexia, an Animal Model of Anorexia Nervosa for Investigating Brain Plasticity Underlying the Gain of Resilience." In *Animal Models of Eating Disorders*, edited by N. Avena, 267–296. Humana. https://doi.org/10.1007/978-1-0716-0924-8_15.

Aoki, C., Y. W. Chen, T. G. Chowdhury, and W. Piper. 2018. "alpha4betadelta-GABAA Receptors in Dorsal Hippocampal CA1 of Adolescent Female Rats Traffic to the Plasma Membrane of Dendritic Spines Following Voluntary Exercise and Contribute to Protection of Animals From Activity-Based Anorexia Through Localization at Excitatory Synapses." *Journal of Neuroscience Research* 96, no. 9: 1450–1466. https://doi.org/10.1002/jnr.24035.

Aoki, C., and A. N. Santiago. 2022. "Pathway-Specific GABAergic Inhibition Contributes to the Gain of Resilience Against Anorexia-Like Behavior of Adolescent Female Mice." *Frontiers in Behavioral Neuroscience* 16: 990354. https://doi.org/10.3389/fnbeh.2022.990354.

APA. 2013. *Diagnostic and Statistical Manual of Mental Disorders DSM-5*. 4th ed. APA.

Arcelus, J., A. J. Mitchell, J. Wales, and S. Nielsen. 2011. "Mortality Rates in Patients With Anorexia Nervosa and Other Eating Disorders. A Meta-Analysis of 36 Studies." *Archives of General Psychiatry* 68, no. 7: 724–731. https://doi.org/10.1001/archgenpsychiatry.2011.74.

Attaallah, B., P. Petitet, R. Zambellas, et al. 2024. "The Role of the Human Hippocampus in Decision-Making Under Uncertainty." *Nature Human Behaviour* 8, no. 7: 1366–1382. https://doi.org/10.1038/s41562-024-01855-2.

Azevedo, E. P., L. Pomeranz, J. Cheng, et al. 2019. "A Role of Drd2 Hippocampal Neurons in Context-Dependent Food Intake." *Neuron* 102, no. 4: 873–886. https://doi.org/10.1016/j.neuron.2019.03.011.

Beadle, J. N., S. Paradiso, M. Brumm, M. Voss, K. Halmi, and L. M. McCormick. 2015. "Larger Hippocampus Size in Women With Anorexia Nervosa Who Exercise Excessively Than Healthy Women." *Psychiatry Research* 232, no. 2: 193–199. https://doi.org/10.1016/j.pscychresns.2014.10.013.

Belmonte, L., N. Achamrah, S. Nobis, et al. 2016. "A Role for Intestinal TLR4-Driven Inflammatory Response During Activity-Based Anorexia." *Scientific Reports* 6: 35813. https://doi.org/10.1038/srep35813.

Berends, T., N. Boonstra, and A. van Elburg. 2018. "Relapse in Anorexia Nervosa: A Systematic Review and Meta-Analysis." *Current Opinion in Psychiatry* 31, no. 6: 445–455. https://doi.org/10.1097/YCO.0000000000000453.

Bergqvist, A. G., J. I. Schall, P. R. Gallagher, A. Cnaan, and V. A. Stallings. 2005. "Fasting Versus Gradual Initiation of the Ketogenic Diet: A Prospective, Randomized Clinical Trial of Efficacy." *Epilepsia* 46, no. 11: 1810–1819. https://doi.org/10.1111/j.1528-1167.2005.00282.x.

Beumont, P. J., B. Arthur, J. D. Russell, and S. W. Touyz. 1994. "Excessive Physical Activity in Dieting Disorder Patients: Proposals for a Supervised Exercise Program." *International Journal of Eating Disorders* 15, no. 1: 21–36. http://www.ncbi.nlm.nih.gov/pubmed/8124324.

Birmingham, C. L., J. Su, J. A. Hlynsky, E. M. Goldner, and M. Gao. 2005. "The Mortality Rate From Anorexia Nervosa." *International Journal of Eating Disorders* 38, no. 2: 143–146. http://www.ncbi.nlm.nih.gov/entrez/query.fcgi?cmd=Retrieve&db=PubMed&dopt=Citation&list_uids=16134111.

Bland, B. H., and S. D. Oddie. 2001. "Theta Band Oscillation and Synchrony in the Hippocampal Formation and Associated Structures: The Case for Its Role in Sensorimotor Integration." *Behavioural Brain Research* 127, no. 1–2: 119–136. https://doi.org/10.1016/s0166-4328(01)00358-8.

Bough, K. J., J. Wetherington, B. Hassel, et al. 2006. "Mitochondrial Biogenesis in the Anticonvulsant Mechanism of the Ketogenic Diet." *Annals of Neurology* 60, no. 2: 223–235. https://doi.org/10.1002/ana.20899.

Buzsaki, G. 2002. "Theta Oscillations in the Hippocampus." *Neuron* 33, no. 3: 325–340. https://doi.org/10.1016/s0896-6273(02)00586-x.

Calabrese, L., B. Scolnick, B. Zupec-Kania, C. Beckwith, K. Costello, and G. K. W. Frank. 2022. "Ketogenic Diet and Ketamine Infusion Treatment to Target Chronic Persistent Eating Disorder Psychopathology in Anorexia Nervosa: A Pilot Study." *Eating and Weight Disorders* 27, no. 8: 3751–3757. https://doi.org/10.1007/s40519-022-01455-x.

Carrera, O., R. A. Adan, E. Gutierrez, et al. 2012. "Hyperactivity in Anorexia Nervosa: Warming Up Not Just Burning-Off Calories." *PLoS One* 7, no. 7: e41851. https://doi.org/10.1371/journal.pone.0041851.

Chen, Y. W., H. Actor-Engel, and C. Aoki. 2018. "α4-GABAA Receptors of Hippocampal Pyramidal Neurons Are Associated With Resilience Against Activity-Based Anorexia for Adolescent Female Mice but Not

for Males." *Molecular and Cellular Neuroscience* 90: 33–48. https://doi.org/10.1016/j.mcn.2018.04.008.

Chowdhury, T. G., G. S. Wable, Y. W. Chen, et al. 2019. "Voluntary Wheel Running Exercise Evoked by Food-Restriction Stress Exacerbates Weight Loss of Adolescent Female Rats but Also Promotes Resilience by Enhancing GABAergic Inhibition of Pyramidal Neurons in the Dorsal Hippocampus." *Cerebral Cortex* 29, no. 10: 4035–4049. https://doi.org/10.1093/cercor/bhy283.

Chowdhury, T. G., G. S. Wable, N. A. Sabaliauskas, and C. Aoki. 2013. "Adolescent Female C57BL/6 Mice With Vulnerability to Activity-Based Anorexia Exhibit Weak Inhibitory Input Onto Hippocampal CA1 Pyramidal Cells." *Neuroscience* 241: 250–267. https://doi.org/10.1016/j.neuroscience.2013.03.020.

Crow, S. J. 2019. "Pharmacologic Treatment of Eating Disorders." *Psychiatric Clinics of North America* 42, no. 2: 253–262. https://doi.org/10.1016/j.psc.2019.01.007.

Dalle Grave, R., S. Calugi, M. El Ghoch, M. Conti, and C. G. Fairburn. 2014. "Inpatient Cognitive Behavior Therapy for Adolescents With Anorexia Nervosa: Immediate and Longer-Term Effects." *Frontiers in Psychiatry* 5: 14. https://doi.org/10.3389/fpsyt.2014.00014.

D'Andrea Meira, I., T. T. Romao, H. J. Pires do Prado, L. T. Kruger, M. E. P. Pires, and P. O. da Conceicao. 2019. "Ketogenic Diet and Epilepsy: What we Know So Far." *Frontiers in Neuroscience* 13: 5. https://doi.org/10.3389/fnins.2019.00005.

Danzer, S. C., and J. O. McNamara. 2004. "Localization of Brain-Derived Neurotrophic Factor to Distinct Terminals of Mossy Fiber Axons Implies Regulation of Both Excitation and Feedforward Inhibition of CA3 Pyramidal Cells." *Journal of Neuroscience* 24, no. 50: 11346–11355. https://doi.org/10.1523/JNEUROSCI.3846-04.2004.

Davis, C., D. K. Katzman, S. Kaptein, et al. 1997. "The Prevalence of High-Level Exercise in the Eating Disorders: Etiological Implications [Research Support, Non-U.S. Gov't]." *Comprehensive Psychiatry* 38, no. 6: 321–326. http://www.ncbi.nlm.nih.gov/pubmed/9406737.

Dellava, J. E., L. M. Thornton, R. M. Hamer, et al. 2010. "Childhood Anxiety Associated With Low BMI in Women With Anorexia Nervosa [Research Support, N.I.H., Extramural Research Support, Non-U.S. Gov't]." *Behaviour Research and Therapy* 48, no. 1: 60–67. https://doi.org/10.1016/j.brat.2009.09.009.

Dilimulati, D., F. Zhang, S. Shao, et al. 2023. "Ketogenic Diet Modulates Neuroinflammation via Metabolites From *Lactobacillus reuteri* After Repetitive Mild Traumatic Brain Injury in Adolescent Mice." *Cellular and Molecular Neurobiology* 43, no. 2: 907–923. https://doi.org/10.1007/s10571-022-01226-3.

Dong, Y., and C. Aoki. 2025. "Subanesthetic Ketamine Ameliorates Activity-Based Anorexia of Adult Mice." *Synapse* 79, no. 1: e70005. https://doi.org/10.1002/syn.70005.

Dong, Y., S. Goodwin-Groen, J. Ma, et al. 2025. "Mechanisms Underlying Sustained Resilience Against Anorexia Nervosa From Sub-Anesthetic Ketamine: An Electron Microscopic Study Using a Mouse Model." *Physiology and Behavior* 298: 114956. https://doi.org/10.1016/physbeh.2025.114956.

Dong, Y., Y. Lin, L. Khatri, H. M. Chao, and C. Aoki. 2024. "Ketogenic Food Ameliorates Activity-Based Anorexia of Adult Female Mice." *International Journal of Eating Disorders* 58: 317–335. https://doi.org/10.1002/eat.24323.

Duncan, L., Z. Yilmaz, H. Gaspar, et al. 2017. "Significant Locus and Metabolic Genetic Correlations Revealed in Genome-Wide Association Study of Anorexia Nervosa." *American Journal of Psychiatry* 174, no. 9: 850–858. https://doi.org/10.1176/appi.ajp.2017.16121402.

Fornaro, M., A. M. Mondin, M. Billeci, et al. 2023. "Psychopharmacology of Eating Disorders: Systematic Review and Meta-Analysis of Randomized Controlled Trials." *Journal of Affective Disorders* 338: 526–545. https://doi.org/10.1016/j.jad.2023.06.068.

Frostad, S., N. Rozakou-Soumalia, S. Darvariu, et al. 2022. "BMI at Discharge From Treatment Predicts Relapse in Anorexia Nervosa: A Systematic Scoping Review." *Journal of Personal Medicine* 12, no. 5: 836–852. https://doi.org/10.3390/jpm12050836.

Fukumoto, K., M. V. Fogaca, R. J. Liu, et al. 2020. "Medial PFC AMPA Receptor and BDNF Signaling Are Required for the Rapid and Sustained Antidepressant-Like Effects of 5-HT(1A) Receptor Stimulation." *Neuropsychopharmacology* 45, no. 10: 1725–1734. https://doi.org/10.1038/s41386-020-0705-0.

Galsworthy-Francis, L., and S. Allan. 2014. "Cognitive Behavioural Therapy for Anorexia Nervosa: A Systematic Review." *Clinical Psychology Review* 34, no. 1: 54–72. https://doi.org/10.1016/j.cpr.2013.11.001.

Goodwin-Groen, S., Y. Dong, and C. Aoki. 2023. "Three Daily Intraperitoneal Injections of Sub-Anesthetic Ketamine Ameliorate Activity-Based Anorexia Vulnerability of Adult Female Mice." *International Journal of Eating Disorders* 57: 1447–1464. https://doi.org/10.1002/eat.24036.

Gorrell, S., and S. B. Murray. 2019. "Eating Disorders in Males." *Child and Adolescent Psychiatric Clinics of North America* 28, no. 4: 641–651. https://doi.org/10.1016/j.chc.2019.05.012.

Gutierrez, E. 2013. "A Rat in the Labyrinth of Anorexia Nervosa: Contributions of the Activity-Based Anorexia Rodent Model to the Understanding of Anorexia Nervosa." *International Journal of Eating Disorders* 46, no. 4: 289–301. https://doi.org/10.1002/eat.22095.

Hartman, A. L., M. Gasior, E. P. Vining, and M. A. Rogawski. 2007. "The Neuropharmacology of the Ketogenic Diet." *Pediatric Neurology* 36, no. 5: 281–292. https://doi.org/10.1016/j.pediatrneurol.2007.02.008.

Hebebrand, J., C. Exner, K. Hebebrand, et al. 2003. "Hyperactivity in Patients With Anorexia Nervosa and in Semistarved Rats: Evidence for a Pivotal Role of Hypoleptinemia [Research Support, Non-U.S. Gov't Review]." *Physiology and Behavior* 79, no. 1: 25–37. http://www.ncbi.nlm.nih.gov/pubmed/12818707.

Hillebrand, J. J., A. A. van Elburg, M. J. Kas, H. van Engeland, and R. A. Adan. 2005. "Olanzapine Reduces Physical Activity in Rats Exposed to Activity-Based Anorexia: Possible Implications for Treatment of Anorexia Nervosa?" *Biological Psychiatry* 58, no. 8: 651–657. http://www.ncbi.nlm.nih.gov/entrez/query.fcgi?cmd=Retrieve&db=PubMed&dopt=Citation&list_uids=16018979.

Huttenlocher, P. R. 1976. "Ketonemia and Seizuers: Metabolic and Anticonvulsant Effects of Two Ketogenic Diets in Childhood Epilepsy." *Pediatric Research* 10: 536–540.

Jiao, Y., Z. Zhang, C. Zhang, et al. 2011. "A Key Mechanism Underlying Sensory Experience-Dependent Maturation of Neocortical GABAergic Circuits In Vivo [Research Support, N.I.H., Extramural Research Support, N.I.H., Intramural]." *Proceedings of the National Academy of Sciences of the United States of America* 108, no. 29: 12131–12136. https://doi.org/10.1073/pnas.1105296108.

Kaye, W. H., J. L. Fudge, and M. Paulus. 2009. "New Insights Into Symptoms and Neurocircuit Function of Anorexia Nervosa." *Nature Reviews. Neuroscience* 10, no. 8: 573–584. https://doi.org/10.1038/nrn2682.

Kepecs, A., and G. Fishell. 2014. "Interneuron Cell Types Are Fit to Function." *Nature* 505, no. 7483: 318–326. https://doi.org/10.1038/nature12983.

Kim, D. Y., K. A. Simeone, T. A. Simeone, et al. 2015. "Ketone Bodies Mediate Antiseizure Effects Through Mitochondrial Permeability Transition." *Annals of Neurology* 78, no. 1: 77–87. https://doi.org/10.1002/ana.24424.

Kim, J. W., K. Suzuki, E. T. Kavalali, and L. M. Monteggia. 2023. "Bridging Rapid and Sustained Antidepressant Effects of Ketamine." *Trends in Molecular Medicine* 29, no. 5: 364–375. https://doi.org/10.1016/j.molmed.2023.02.003.

Kinzig, K. P., M. A. Honors, S. L. Hargrave, B. M. Davenport, A. D. Strader, and D. Wendt. 2010. "Sensitivity to the Anorectic Effects of Leptin Is Retained in Rats Maintained on a Ketogenic Diet Despite Increased Adiposity [Research Support, N.I.H., Extramural]." *Neuroendocrinology* 92, no. 2: 100–111. https://doi.org/10.1159/000314180.

Klenotich, S. J., and S. C. Dulawa. 2012. "The Activity-Based Anorexia Mouse Model." *Methods in Molecular Biology* 829: 377–393. https://doi.org/10.1007/978-1-61779-458-2_25.

Korte, M., H. Kang, T. Bonhoeffer, and E. Schuman. 1998. "A Role for BDNF in the Late-Phase of Hippocampal Long-Term Potentiation." *Neuropharmacology* 37, no. 4–5: 553–559. https://doi.org/10.1016/s0028-3908(98)00035-5.

Kossoff, E. H., B. A. Zupec-Kania, S. Auvin, et al. 2018. "Optimal Clinical Management of Children Receiving Dietary Therapies for Epilepsy: Updated Recommendations of the International Ketogenic Diet Study Group." *Epilepsia Open* 3, no. 2: 175–192. https://doi.org/10.1002/epi4.12225.

Kron, L., J. L. Katz, G. Gorzynski, and H. Weiner. 1978. "Hyperactivity in Anorexia Nervosa: A Fundamental Clinical Feature." *Comprehensive Psychiatry* 19, no. 5: 433–440. http://www.ncbi.nlm.nih.gov/pubmed/679677.

Krystal, J. H., E. T. Kavalali, and L. M. Monteggia. 2024. "Ketamine and Rapid Antidepressant Action: New Treatments and Novel Synaptic Signaling Mechanisms." *Neuropsychopharmacology* 49, no. 1: 41–50. https://doi.org/10.1038/s41386-023-01629-w.

Li, J., R. Temizer, Y. W. Chen, and C. Aoki. 2024. "Ketamine Ameliorates Activity-Based Anorexia of Adolescent Female Mice Through Changes in GluN2B-Containing NMDA Receptors at Postsynaptic Cytoplasmic Locations of Pyramidal Neurons and Interneurons of Medial Prefrontal Cortex." *Brain Structure & Function* 229, no. 2: 323–348. https://doi.org/10.1007/s00429-023-02740-w.

Li, J. Y., T. B. Kuo, I. T. Hsieh, and C. C. Yang. 2012. "Changes in Hippocampal Theta Rhythm and Their Correlations With Speed During Different Phases of Voluntary Wheel Running in Rats." *Neuroscience* 213: 54–61. https://doi.org/10.1016/j.neuroscience.2012.04.020.

Liu, H., Y. Yang, Y. Wang, et al. 2018. "Ketogenic Diet for Treatment of Intractable Epilepsy in Adults: A Meta-Analysis of Observational Studies." *Epilepsia Open* 3, no. 1: 9–17. https://doi.org/10.1002/epi4.12098.

Marty, S., P. Carroll, A. Cellerino, et al. 1996. "Brain-Derived Neurotrophic Factor Promotes the Differentiation of Various Hippocampal Nonpyramidal Neurons, Including Cajal-Retzius Cells, in Organotypic Slice Cultures." *Journal of Neuroscience* 16, no. 2: 675–687. https://doi.org/10.1523/JNEUROSCI.16-02-00675.1996.

McFarlane, T., M. P. Olmsted, and K. Trottier. 2008. "Timing and Prediction of Relapse in a Transdiagnostic Eating Disorder Sample." *International Journal of Eating Disorders* 41, no. 7: 587–593. http://www.ncbi.nlm.nih.gov/entrez/query.fcgi?cmd=Retrieve&db=PubMed&dopt=Citation&list_uids=18473336.

Mehler, P. S., and C. Brown. 2015. "Anorexia Nervosa – Medical complications." *Journal of Eating Disorders* 3: 11. https://doi.org/10.1186/s40337-015-0040-8.

Modlinska, K., R. Stryjek, and W. Pisula. 2015. "Food Neophobia in Wild and Laboratory Rats (Multi-Strain Comparison)." *Behavioural Processes* 113: 41–50. https://doi.org/10.1016/j.beproc.2014.12.005.

Mulkens, S., and G. Waller. 2021. "New Developments in Cognitive-Behavioural Therapy for Eating Disorders (CBT-ED)." *Current Opinion in Psychiatry* 34, no. 6: 576–583. https://doi.org/10.1097/YCO.0000000000000745.

Norwitz, N. G., M. Hurn, and F. E. Forcen. 2023. "Animal-Based Ketogenic Diet Puts Severe Anorexia Nervosa Into Multi-Year Remission: A Case Series." *Journal of Insulin Resistance* 6, no. 1: 8. https://doi.org/10.4102/jir.v6i1.84.

Panja, D., and C. R. Bramham. 2014. "BDNF Mechanisms in Late LTP Formation: A Synthesis and Breakdown." *Neuropharmacology* 76: 664–676. https://doi.org/10.1016/j.neuropharm.2013.06.024.

Paoli, A., A. Bianco, T. Moro, J. F. Mota, and C. F. Coelho-Ravagnani. 2023. "The Effects of Ketogenic Diet on Insulin Sensitivity and Weight Loss, Which Came First: The Chicken or the Egg?" *Nutrients* 15, no. 14: 1–32. https://doi.org/10.3390/nu15143120.

Pisetsky, D. S., S. E. Trace, K. A. Brownley, et al. 2014. "The Expression of Cytokines and Chemokines in the Blood of Patients With Severe Weight Loss From Anorexia Nervosa: An Exploratory Study." *Cytokine* 69, no. 1: 110–115. https://doi.org/10.1016/j.cyto.2014.05.018.

Polito, R., M. E. La Torre, F. Moscatelli, et al. 2023. "The Ketogenic Diet and Neuroinflammation: The Action of Beta-Hydroxybutyrate in a Microglial Cell Line." *International Journal of Molecular Sciences* 24, no. 4: 3102. https://doi.org/10.3390/ijms24043102.

Reyes-Ortega, P., D. Ragu Varman, V. M. Rodriguez, and D. Reyes-Haro. 2020. "Anorexia Induces a Microglial Associated Pro-Inflammatory Environment and Correlates With Neurodegeneration in the Prefrontal Cortex of Young Female Rats." *Behavioural Brain Research* 392: 112606. https://doi.org/10.1016/j.bbr.2020.112606.

Routtenberg, A., and A. W. Kuznesof. 1967. "Self-Starvation of Rats Living in Activity Wheels on a Restricted Feeding Schedule." *Journal of Comparative and Physiological Psychology* 64, no. 3: 414–421. http://www.ncbi.nlm.nih.gov/pubmed/6082873.

Schmalbach, I., B. Herhaus, S. Passler, et al. 2020. "Cortisol Reactivity in Patients With Anorexia Nervosa After Stress Induction." *Translational Psychiatry* 10, no. 1: 275. https://doi.org/10.1038/s41398-020-00955-7.

Scolnick, B., B. Zupec-Kania, L. Calabrese, C. Aoki, and T. Hildebrandt. 2020. "Remission From Chronic Anorexia Nervosa With Ketogenic Diet and Ketamine: Case Report." *Frontiers in Psychiatry* 11: 763. https://doi.org/10.3389/fpsyt.2020.00763.

Shen, H., Q. H. Gong, C. Aoki, et al. 2007. "Reversal of Neurosteroid Effects at alpha4beta2delta GABAA Receptors Triggers Anxiety at Puberty." *Nature Neuroscience* 10, no. 4: 469–477. http://www.ncbi.nlm.nih.gov/entrez/query.fcgi?cmd=Retrieve&db=PubMed&dopt=Citation&list_uids=17351635.

Shen, H., Q. H. Gong, M. Yuan, and S. S. Smith. 2005. "Short-Term Steroid Treatment Increases Delta GABAA Receptor Subunit Expression in Rat CA1 Hippocampus: Pharmacological and Behavioral Effects." *Neuropharmacology* 49, no. 5: 573–586. http://www.ncbi.nlm.nih.gov/entrez/query.fcgi?cmd=Retrieve&db=PubMed&dopt=Citation&list_uids=15950994.

Shen, H., N. Sabaliauskas, A. Sherpa, et al. 2010. "A Critical Role for alpha4betadelta GABAA Receptors in Shaping Learning Deficits at Puberty in Mice." *Science* 327, no. 5972: 1515–1518. http://www.ncbi.nlm.nih.gov/entrez/query.fcgi?cmd=Retrieve&db=PubMed&dopt=Citation&list_uids=20299596.

Sleiman, S. F., J. Henry, R. Al-Haddad, et al. 2016. "Exercise Promotes the Expression of Brain Derived Neurotrophic Factor (BDNF) Through the Action of the Ketone Body Beta-Hydroxybutyrate." *eLife* 5: e15092. https://doi.org/10.7554/eLife.15092.

Smith, A. R., K. L. Zuromski, and D. R. Dodd. 2018. "Eating Disorders and Suicidality: What We Know, What We Don't Know, and Suggestions for Future Research." *Current Opinion in Psychology* 22: 63–67. https://doi.org/10.1016/j.copsyc.2017.08.023.

Sosa, M., and L. M. Giocomo. 2021. "Navigating for Reward." *Nature Reviews. Neuroscience* 22, no. 8: 472–487. https://doi.org/10.1038/s41583-021-00479-z.

Steinglass, J. E., S. C. Kaplan, Y. Liu, Y. Wang, and B. T. Walsh. 2014. "The (Lack of) Effect of Alprazolam on Eating Behavior in Anorexia Nervosa: A Preliminary Report." *International Journal of Eating Disorders* 47, no. 8: 901–904. https://doi.org/10.1002/eat.22343.

Tanner, G. R., A. Lutas, J. R. Martinez-Francois, and G. Yellen. 2011. "Single K ATP Channel Opening in Response to Action Potential Firing in Mouse Dentate Granule Neurons." *Journal of Neuroscience* 31, no. 23: 8689–8696. https://doi.org/10.1523/JNEUROSCI.5951-10.2011.

Temizer, R., Y.-W. Chen, and C. Aoki. 2023. "Individual Differences in the Positive Outcome From Adolescent Ketamine Treatment in a Female Mouse-Model of Anorexia Nervosa Involves Drebrin A at Excitatory Synapses of the Medial Prefrontal Cortex." *Synapse* 77, no. 1: 19. https://doi.org/10.1002/syn.22253.

Vining, E. P., J. M. Freeman, K. Ballaban-Gil, et al. 1998. "A Multicenter Study of the Efficacy of the Ketogenic Diet." *Archives of Neurology* 55, no. 11: 1433–1437. https://doi.org/10.1001/archneur.55.11.1433.

Wable, G. S., N. C. Barbarich-Marsteller, T. G. Chowdhury, N. A. Sabaliauskas, C. R. Farb, and C. Aoki. 2014. "Excitatory Synapses on Dendritic Shafts of the Caudal Basal Amygdala Exhibit Elevated Levels of GABAA Receptor alpha4 Subunits Following the Induction of Activity-Based Anorexia." *Synapse* 68, no. 1: 1–15. https://doi.org/10.1002/syn.21690.

Wable, G. S., Y. W. Chen, S. Rashid, and C. Aoki. 2015. "Exogenous Progesterone Exacerbates Running Response of Adolescent Female Mice to Repeated Food Restriction Stress by Changing alpha4-GABAA Receptor Activity of Hippocampal Pyramidal Cells." *Neuroscience* 310: 322–341. https://doi.org/10.1016/j.neuroscience.2015.09.006.

Wable, G. S., J. Y. Min, Y. W. Chen, and C. Aoki. 2015. "Anxiety Is Correlated With Running in Adolescent Female Mice Undergoing Activity-Based Anorexia." *Behavioral Neuroscience* 129, no. 2: 170–182. https://doi.org/10.1037/bne0000040.

Walsh, B. T. 2013. "The Enigmatic Persistence of Anorexia Nervosa." *American Journal of Psychiatry* 170, no. 5: 477–484. https://doi.org/10.1176/appi.ajp.2012.12081074.

Watson, H. J., Z. Yilmaz, L. M. Thornton, et al. 2019. "Genome-Wide Association Study Identifies Eight Risk Loci and Implicates Metabo-Psychiatric Origins for Anorexia Nervosa." *Nature Genetics* 51, no. 8: 1207–1214. https://doi.org/10.1038/s41588-019-0439-2.

Wei, S. J., J. R. Schell, E. S. Chocron, et al. 2024. "Ketogenic Diet Induces p53-Dependent Cellular Senescence in Multiple Organs." *Science Advances* 10, no. 20: eado1463. https://doi.org/10.1126/sciadv.ado1463.

Wilder, R. M. 1921. "The Effect of Ketonemia on the Course of Epilepsy." *Mayo Clinic Proceedings* 2: 307–308.

Supporting Information

Additional supporting information can be found online in the Supporting Information section. **Figure S1:** EM analysis reveals unchanging composition of synapse types in SLM of KGD, compared to SD. Unpaired two-way t-test results show lack of differences across the KGD versus SD groups, comparing the areal density of I-to-I (a), I-to-E (c), E-to-I (e) and E-to-E (f) synapses in the SLM. The proportion of all GABAergic axons engaged in I-to-I (b) and I-to-E (d) synapses are also shown to not differ across the groups (panels b, d and f).